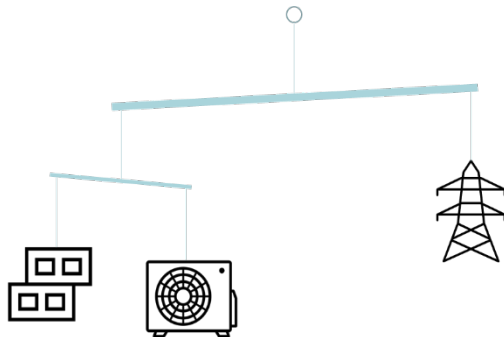


The Evolving Carbon Balance of High-Performance Buildings



By

Adam Yarnell

Bachelor of Arts in Environmental Studies, Brown University, 2011

Submitted in partial fulfillment of the requirements for the degree of

**Master in Design Studies
Energy and Environment**

At the Harvard University Graduate School of Design

May, 2022

Copyright © 2022 by Adam Yarnell

The author hereby grants Harvard University permission to reproduce and distribute copies of this Final Project, in whole or in part for educational purposes.

Signature of the Author _____ 

Adam Yarnell
Harvard University Graduate School of Design

Certified by _____ 

Jonathan Grinham
Lecturer in Architecture
Harvard University Graduate School of Design

Table of Contents

I.	Introduction	1
a.	Theoretical Background	1
II.	Literature Review.....	2
III.	Methodology.....	3
a.	Operational Carbon	7
b.	Embodied Carbon.....	11
c.	Refrigerants	12
d.	Summary	13
IV.	Results	15
V.	Discussion.....	24
VI.	Conclusions.....	25
VII.	References.....	27
VIII.	Appendix	
A.	Refrigerant Impacts	
B.	Decarbonization Scenarios	
C.	Miscellanea.....	

Tables

Table 1: Key properties of case study building.....	3
Table 2: PHIUS performance and design requirements.....	4
Table 3: ASHRAE 90.1-2004 prescriptive design requirements.....	5
Table 4: Specifications of four principal energy simulation cases: a) Base case – ASHRAE 90.1-2004 b) Regenerative Mode – Code envelope with PHIUS equipment c) Conservative Mode – PHIUS envelope with code equipment d) Combined – PHIUS envelope and equipment.....	7
Table 5: Initial grid intensities of U.S.-Average and relevant eGRID subregions	10
Table 6: List of five data filters and available options that can be used to generate 192 different life-cycle carbon comparison charts.	13
Table 7: Properties of analyzed systems for refrigerant impact study.....	Appx. A
Table 8: Leakage and EOL loss assumptions for a) air-source heat pump and heat pump water heater and b) split air conditioning system.....	Appx. A
Table 9: Life-cycle impacts per specified refrigerant.....	Appx. A
Table 10: ENERGY STAR equipment for a) higher-internal-loads cases ("PHIUS – Inefficient High EC") and b) low-internal-loads cases ("PHIUS - Efficient Low EC", "PHIUS - Efficient Standard EC", and "PHIUS - Efficient High EC")	Appx. C

Figures

Figure 1: Adapted images from (Banham, 1984) showing two different historical approaches to shelter. In a) the traditional case, the carbon needed to sustain the fire is much greater than that needed to build the tent. In b) the high-efficiency case, the smaller and cleaner-burning fire actually emits less carbon over its lifetime than the embodied carbon in the tentpoles and canvas.	2
Figure 2: 3D model of case study building, courtesy of Gowri et al. (2007).....	3
Figure 3: Map of reference cities with climatic summaries.....	4
Figure 4: Diagrams of four principal energy simulation cases: a) Base case – ASHRAE 90.1-2004 b) Regenerative Mode – Code envelope with PHIUS equipment c) Conservative Mode – PHIUS envelope with code equipment d) Combined – PHIUS envelope and equipment. All diagrams were laid out by Adam Yarnell and executed by Bianca Seong.	8
Figure 5: Cumulative emissions six decarbonization scenarios applied to the eGRID US-Average.....	10
Figure 6: LCA data quality. Percentages are based on the number of components with individual data sources across all eight cases.....	11
Figure 7: Key inherited changes in constructing code cases (above) and Passive House cases (below)....	13
Figure 8: Box and whiskers plot of the reference scenario. The table on the left lists the selected data filters, and the legend above shows the most important attributes of each case.....	15
Figure 9: Average life-cycle emissions for the eight case (four code, four Passive House) using the reference scenario data filters.....	16
Figure 10: Reference scenario comparison of the lowest-emitting code case and highest-emitting Passive House case using initial grid intensities set to a) the U.S. average and b) specific regional grids.....	17
Figure 11: Comparison of gas and electric cases with a) a high-carbon electric grid and b) a rapidly decarbonized grid.	18
Figure 12: Comparison of a low-embodied-carbon code case with Passive House cases in a) moderate and b) idealized scenarios.....	20
Figure 13: Relative contribution of MEP equipment (embodied carbon and refrigerants) to life-cycle emissions in a rapidly-decarbonized scenario.	22
Figure 14: Relative contribution of refrigerants to life-cycle emissions in a high impact scenario.....	23
Figure 15: Annual grid emissions (kgCO ₂ e/kWh consumed) for an eGRID average grid (US-Average) and four subregions for six decarbonization scenarios: a) business-as-usual b) 50% by 2050 c) 80% by 2050 d) 100% by 2050 e) 80% by 2035, 100% by 2050 f) 100% by 2035.....	Appx. B
Figure 16: Figure 16: Decision map for the eight life-cycle emissions cases in the study.....	Appx. C

Acknowledgments

The author wishes to express sincere thanks to Jonathan Grinham for concept development, research support, and mentorship. He also recognizes Les Norford for providing technical assistance, engaging discussions, and hospitality in 5-414. A special thank you to Bianca Seong for graphical, and, more importantly, emotional support. Kate Doherty, Robb Aldrich, and Thomas Moore of Steven Winter Associates all provided important technical assistance, and Kate, in particular, offered invaluable help constructing realistic passive house cases. The author also acknowledges the Harvard Joint Center for Housing Studies for a generous thesis grant. Finally, the author would like to thank Laurie and Gary Yarnell for decades of love and support.

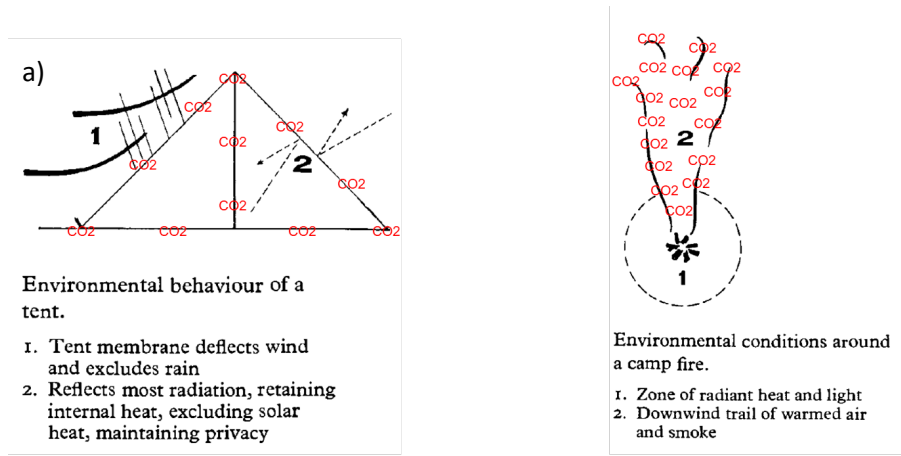
Abstract

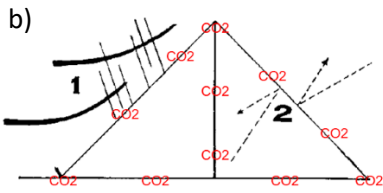
Highly operationally-efficient buildings typically require significant embodied flows to guarantee low energy consumption. To highlight this tension, an operational energy simulation of a prototypical mid-rise apartment was equipped with all-electric heating, ventilation, and air conditioning (HVAC) systems. The building was then upgraded from the comparatively under-performing ASHRAE 90.1-2004 standard to the higher-performing PHIUS 2021 certification, while the grid that supplied the building was simulated with aggressive, moderate, and business-as-usual emissions intensity scenarios. To assess life-cycle impacts, changes to the building's structure, foundation, enclosure, and mechanical equipment were evaluated using life-cycle assessment (LCA), and refrigerant impacts were calculated separately using a range of 100-year global warming potentials (GWP) and leakage assumptions. In the end, the ranking of optimal high-performance building strategies is sensitive to different combinations of grid, refrigerant, and carbon accounting assumptions. As an example, the results suggest that, given a rapidly decarbonized grid, operationally-inefficient buildings with low-embodied-carbon materials will emit less life-cycle carbon than certain low-energy buildings with standard materials.

I. Introduction

This thesis attempts to determine the life-cycle impacts of different high-performance building strategies. First, key precedents and relevant literature are reviewed and discussed. In the Methodology section, a detailed building case study is established. Base building properties and climate zones are described, and the mechanics of the three linked carbon analyses are expounded. Ultimately, the embedded case study presents a total of 6144 cases: eight buildings in four climate zones with two electricity grids, six electricity decarbonization scenarios, two treatments of biogenic carbon, four refrigerant impact scenarios, and two HVAC sizing scenarios. The Results section extracts relevant statistics, and the Discussion section addresses limitations of this work and future directions that can be pursued. Finally, a Conclusions section interprets the findings.

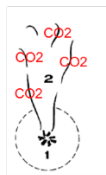
a. Theoretical Background





Environmental behaviour of a tent.

1. Tent membrane deflects wind and excludes rain
2. Reflects most radiation, retaining internal heat, excluding solar heat, maintaining privacy



Environmental conditions around a camp fire.

1. Zone of radiant heat and light
2. Downwind trail of warmed air and smoke

Conservative Mode

Regenerative Mode

Figure 1: Adapted images from (Banham, 1984) showing two different historical approaches to shelter. In a) the traditional case, the carbon needed to sustain the fire is much greater than that needed to build the tent. In b) the high-efficiency case, the smaller and cleaner-burning fire actually emits less carbon over its lifetime than the embodied carbon in the tentpoles and canvas.

In *Architecture of the Well-Tempered Environment* (Banham, 1984), Reyner Banham splits architectural history into two domains (Fig. 1). Conservative Mode structures rely on passive means to regulate climate, while Regenerative Mode structures employ active energy inputs to condition space. Bioclimatic designers have favored the Conservative Mode, as, historically, far more cords of wood were needed for the fire than for tent poles. Today, these campfires are burning more efficiently and cleanly, but the tents still require roughly the same amount of wood to manufacture.

II. Literature Review

Traditionally, researchers have studied buildings' operational and embodied impacts in isolation; operational energy has been measured through metering or simulation, while embodied energy has been evaluated with life-cycle assessment (LCA). Although select investigators compared direct and indirect building emissions in the 1970s (Hannon et al., 1976) and 1980s (Connaughton, 1987), comprehensive research linking these two domains did not appear prominently until the 1990s (Cole & Rousseau, 1992; Pullen & Perkins, 1995). Comparisons of operational and embodied carbon justified a narrow focus on the former, as typical building operation was shown to generate upwards of 80% of total life-cycle energy (Cole & Kernan, 1996). Subsequent studies have supported this conclusion, albeit with the intuitive caveat that better operational performance will drive up the proportion of embodied carbon (Fay et al., 2000; Scheuer et al., 2003; Ramesh et al., 2010; Hernandez & Kenny, 2011; Ibn-Mohammed et al., 2013; Azari & Abbasabadi, 2018). Even if building physics are held constant, the ratio of embodied to operational carbon also increases as buildings are electrified and connect to cleaner grids (Stephan et al., 2013; Chastas et al., 2016; Grinham et al., 2022). Research further suggests that lowering operational emissions will tend to increase absolute embodied emissions (Kneifel et al., 2018), and pursuing sufficiently-high performance may actually increase total emissions compared to conventional alternatives (Stephan et al., 2013; Copiello, 2017). Replacing carbon-intensive materials with lower-carbon alternatives, however, can limit this increase in embodied carbon (Thormark, 2006; Pomponi & Moncaster, 2016).

The embodied carbon impacts of mechanical, electrical, and plumbing (MEP) equipment, however, are treated inconsistently in the analyses above. Despite Cole & Kernan's finding that MEP equipment can constitute roughly one-third of total embodied emissions (1996), whole-building LCAs typically exclude heating, ventilation, and air conditioning (HVAC) and miscellaneous equipment (Simonen et al., 2017; Dixit, 2019). More contemporary research estimates that HVAC equipment contributes in the range of 11-15% to total initial embodied carbon (Rodriguez et al., 2020). Studies also suggest that direct refrigerant emissions constitute a significant portion of total HVAC-related emissions (Beshr et al., 2017; Wan et al., 2021), and refrigerant emissions can actually outstrip operational emissions in extreme cases (George et al., 2019). Finally, although HVAC systems are sized to peak loads, only two papers were found that explored the life-cycle impacts of HVAC sizing in a buildings context (Phillips et al., 2020; Hein et al., 2021) (Hein et al., 2021).

III. Methodology

Table 1: Key properties of case study building.

Typology	Multifamily
Floors	4
Units	31 DU, 1 office
Floor Area (m ²)	3131
iCFA (m ²)	2901
Form	Rectangular; 46.3 x 16.9m
WWR	20%, all faces
Floor-to-Floor Height (m)	3.05
Floor Construction	203mm concrete slabs with steel columns and beams
Exterior wall construction	Steel-frame walls (48x98mm, 400mm o.c.): Stucco, building wrap, 16mm GWB, Steel studs and cavity insulation, 16mm GWB
Roof construction	Built-up roof: gravel-ballasted asphaltic membrane, insulation, metal decking

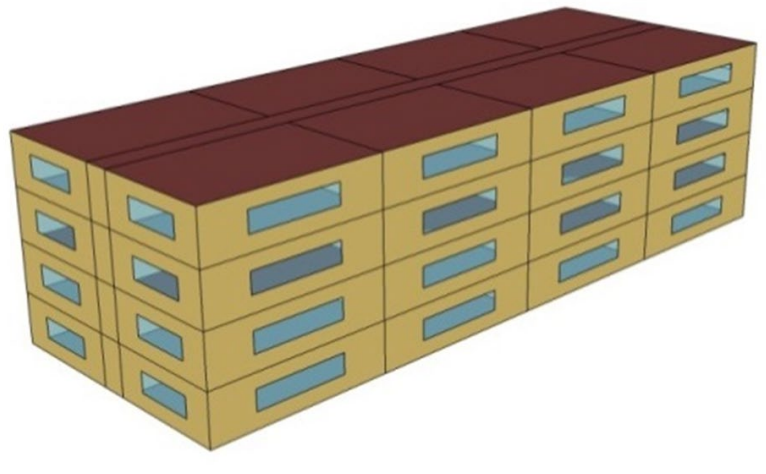


Figure 2: 3D model of case study building, courtesy of Gowri et al. (2007)

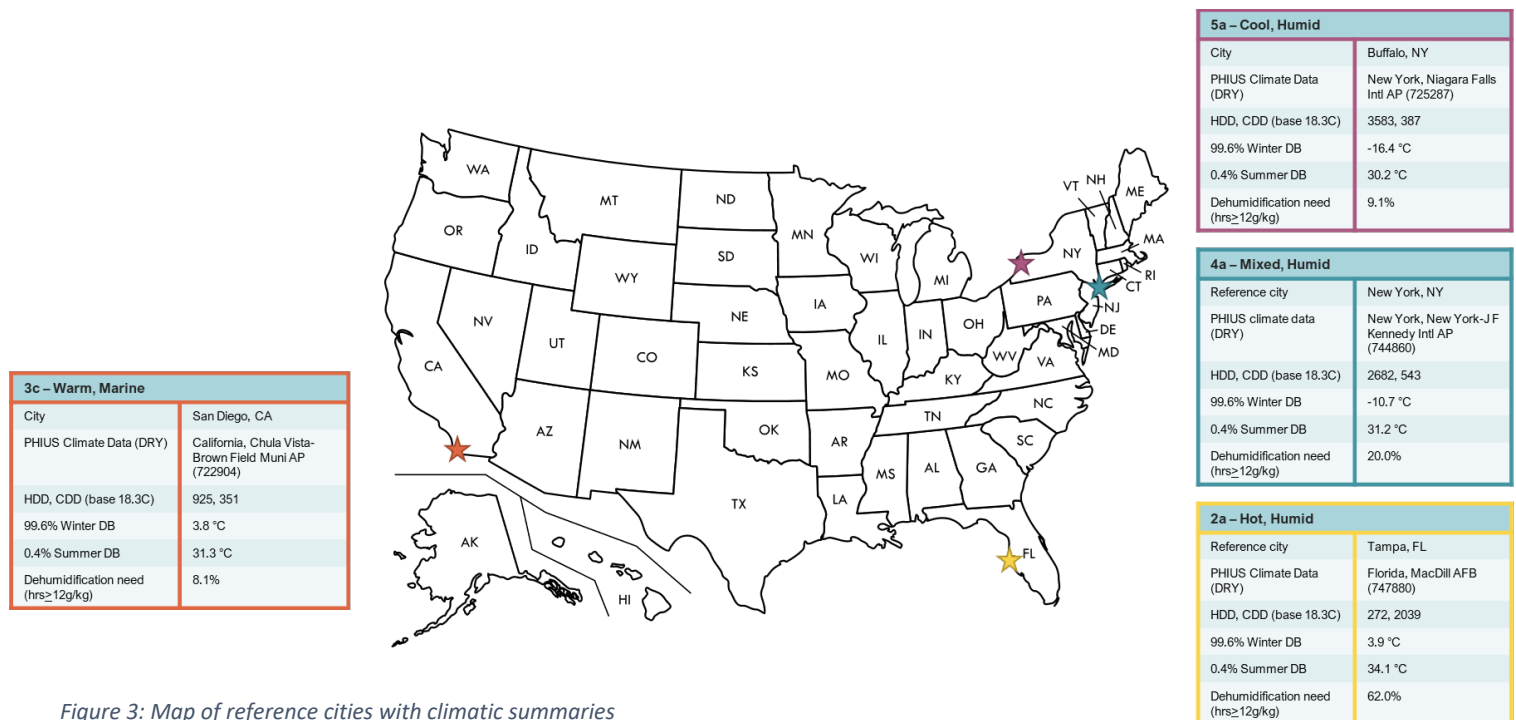


Figure 3: Map of reference cities with climatic summaries

Case studies were proposed to evaluate the life-cycle carbon intensity of Conservative Mode architecture. The focus was narrowed to new construction in order to study full cradle-to-grave impacts; the estimated global need for 200 billion square meters of additional floor area by 2060 (Abergel et al., 2017) provided further justification. Residential construction was also favored over commercial due to the former's dominance of building-related energy consumption (U.S. Energy Information Administration (EIA), 2022). Within the residential sector, the midrise multifamily typology was selected both for its applicability to mid-density urbanization and its comparability with commercial typologies. Ultimately, the U.S. Department of Energy's "Mid-rise Apartment" prototype building model (Goel et al., 2014) was chosen for the case study (*Fig. 2*). Using the DOE's model also increases the replicability and comparability of the simulations as the performance of these buildings is already well understood and highly cited in literature. Finally, four unique climates, per Venkatraj et al. (2020), were designated in order to initiate a sensitivity study (*Fig. 3*). Climate variability produces load variability, which in turn provides a useful filter for assessing embodied impacts from HVAC systems. Hot and humid Tampa puts strain on cooling and dehumidification, cooler New York and Buffalo stress heating systems, and San Diego offers a mild climate as a control.

Table 2: PHIUS performance and design requirements

PHIUS 2021	2A	3C	4A	5A
Annual Heating Demand (kWh/m ² /yr) (PHIUS+ 2018)	3.2	5.1	11.1	13.9
Annual Cooling Demand (kWh/m ² /yr) (PHIUS+ 2018)	72.5	28.2	24	16.6
Peak Heating Load (W/m ²) (PHIUS+ 2018)	5.7	5.1	10.3	11.8

Peak Cooling Load (W/m ²) (PHIUS+ 2018)	10	6.3	7.2	6.9
kWh/person/yr (PHIUS+ 2018)	3840			
Envelope Airtightness (m ³ /m ² h at 50pa)	0.9			
Windows	ENERGY STAR certified or triple-glazed with thermally broken frames			
Lighting	80% of fixtures or bulbs ENERGY STAR qualified			
Appliances	ENERGY STAR qualified refrigerators, dishwashers, and clothes washers			

Table 3: ASHRAE 90.1-2004 prescriptive design requirements

ASHRAE 90.1-04	2A	3C	4A	5A
Roof - Minimum R-Value	RSI 2.64 (R-15) c.i.			
Walls (Wood-Framed) - Minimum R-Value	RSI 2.29 (R-13)			
Walls (Steel-Framed) - Minimum R-Value	RSI 2.29 (R-13)	RSI 2.29 (R-13) + RSI 0.67 (R-3.8 c.i.)	RSI 2.29 (R-13) + RSI 1.32 (R-7.5 c.i.)	RSI 2.29 (R-13) + RSI 1.32 (R-7.5 c.i.)
Slab-on-grade (Unheated) - Minimum R-Value	NR			
Opaque Doors (Swinging) - Maximum U-Value	3.97 USI (0.7 IP)			
Operable Glazing - Maximum U-Value	7.21 USI (1.27 IP)	7.21 USI (1.27 IP)	3.80 USI (0.67 IP)	3.80 USI (0.67 IP)
All faces - Maximum SHGC	0.25	0.61	0.39	0.39
Duct Insulation - Exterior - Minimum R-Value	RSI 1.06 (R-6)			
Economizer - Required if individual System Cooling Capacity \geq BTU/h	NR	325000 (95 kW)	NR	675000 (198 kW)
Fan Power Limitation	<20,000 cfm (33,980 m ³ /h); 1.2 hp/1000 cfm (526 W/1000 m ³ /h)			

Minimum SEER	Based on capacity and system type: 10-12			
Minimum HSPF	Based on capacity and system type: 6.8-7.4			
Exhaust Air Energy Recovery	50% recovery effectiveness for systems >5000 cfm (8496 m ³ /h) and >70% OA; cooling only	NR	50% recovery effectiveness for systems >5000 cfm (8496 m ³ /h) and >70% OA	50% recovery effectiveness for systems >5000 cfm (8496 m ³ /h) and >70% OA

Next, one must find meaningful performance proxies for both Conservative Mode and Regenerative Mode buildings. Passive house provides a perfect Conservative Mode model. All passive house requirements are designed to ensure as little useful heat as possible escapes the building. This study uses PHIUS, which is a U.S.-adapted version of the original German standard. Here, the American standard offers two main benefits: heating and cooling requirements are adapted to specific climates; and verification software is provided to the public for free. The 2021 version of the standard (PHIUS, 2021c) was used to build out all cases, but more restrictive heating and cooling limits were sourced from the 2018 standard (PHIUS, 2019) in order to fix a stronger constraint. Relevant PHIUS requirements are listed in *Tbl. 2*. The goal for the Regenerative Mode case was to model a poor-performing but still feasible building. A sufficiently high operational baseline forces one to lean heavily on the embodied carbon lever to effect life cycle carbon reductions. ASHRAE 90.1-2004 (ANSI/ASHRAE/IES, 2004)—the first update of the 90.1 energy standard—is the earliest statewide energy code still in use and, therefore, provides a suitable framework. As seen in *Tbl. 3*, only minimal insulation, moderate-performance glazing, and basic HVAC efficiency measures are required by the standard. This 2004 version, in fact, represents a 27% increase in site energy consumption over the current 2019 standard (Halverson, Liu, et al., 2010) (Halverson, Williamson, et al., 2010) (Halverson et al., 2014) (Athalye et al., 2017) (Zhang et al., 2021).

Three independent workflows were linked to compute life-cycle carbon expenditures of the case study: operational energy simulation, life-cycle assessment, and refrigerant impact analysis. *Eq. 1*, partially adapted from (Akbarnezhad & Xiao, 2017), details the life-cycle emissions calculation employed in this thesis.

$$LCCO2_k = \sum \left(\frac{MJ}{yr} * f_k * SL_k \right) + \sum_j (Q_j * f_j) + RI_k \quad (1)$$

Where, LCCO2: Life-cycle carbon emissions

k: Studied building

MJ/yr: Annual site energy consumption

f_k: Grid emissions intensity (kgCO₂e/kWh)

SL_k: Service life of building (yrs)

j: building component

Q_j: Mass of building component (kg)

f_j: Embodied carbon factor of material (kgCO₂e/kg)

RI_k: Refrigerant impact of studied building (kgCO₂e) (*Eq. 2*)

a. Operational Carbon

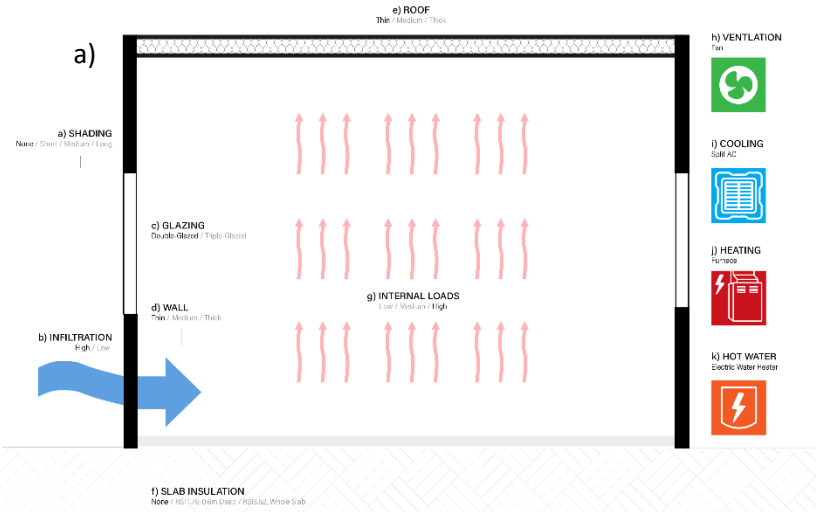


Table 4: Specifications of four principal energy simulation cases:
a) Base case – ASHRAE 90.1-2004 b) Regenerative Mode – Code envelope with PHIUS equipment c) Conservative Mode – PHIUS

Metric	Value	Source
a. Shading (South Façade)	None	Goel, 2014 (PNNL)
b. Infiltration	14 m³/m²h at 50pa (6 ACH50)	Gordon, 2013 (PNNL)
c. Glazing	Double-pane; U-value: 1.26-6.98 W/m²K; SHGC: 0.25-0.61	Goel, 2014 (PNNL); Kneifel, 2019 (BIRDS)
d. Wall Insulation	RSI 2.29 stud; RSI 0.67-1.32 CI (3c, 4a, 5a)	Goel, 2014 (PNNL)
e. Roof Insulation	RSI 2.64 CI	Goel, 2014 (PNNL)
f. Slab Insulation	None	Goel, 2014 (PNNL)
g. Internal Loads	High (5.2-5.3 W/m²)	Goel, 2014 (PNNL); PHIUS, n.d.b
h. Ventilation	Duct fan (no heat recovery)	Goel, 2014 (PNNL); Lstiburek, 2006
i. Cooling	Split air conditioning (3.22 gross rated COP)	Goel, 2014 (PNNL)
j. Heating	Furnace (80% efficiency)	Goel, 2014 (PNNL)
k. Hot Water	Electric water heater with 200L storage	Goel, 2014 (PNNL)

Metric	Value	Source
a. Shading (South Façade)	0.42 PF (2a); None (3c, 4a, 5a)	PHIUS, 2021b
b. Infiltration	0.9 m³/m²h at 50pa (0.4 ACH50)	PHIUS, 2021c
c. Glazing	Triple-pane; U-value: 0.80-1.54 W/m²K; SHGC: 0.19-0.56	PHIUS, 2021c; PHIUS, n.d.-a
d. Wall Insulation	RSI 2.29 stud; RSI 0.67-1.32 CI (2a, 4a)	ASHRAE 90.1-2004; ASHRAE 90.1-2019
e. Roof Insulation	RSI 2.64-5.28	ASHRAE 90.1-2004; ASHRAE 90.1-2019
f. Slab Insulation	None (2a, 3c); RSI 2.5 for 0.6m (4a); RSI 1.75 for 0.6m (5a)	PHIUS 2021c; PHIUS, 2021b
g. Internal Loads	Low (1.8-3.6 W/m²)	PHIUS, n.d.b; ENERGY STAR (n.d.)
h. Ventilation	ERV (2a); Duct fan (no heat recovery) (3c); HRV (4a, 5a)	PHIUS, 2021a
i. Cooling	ASHP (33.1 SEER)	Mitsubishi Electric, 2016
j. Heating	ASHP (4.68@8C COP)	Mitsubishi Electric, 2016
k. Hot Water	HPWH (2a, 3c, 5a); tankless electric water heater (4a)	PHIUS, 2021d

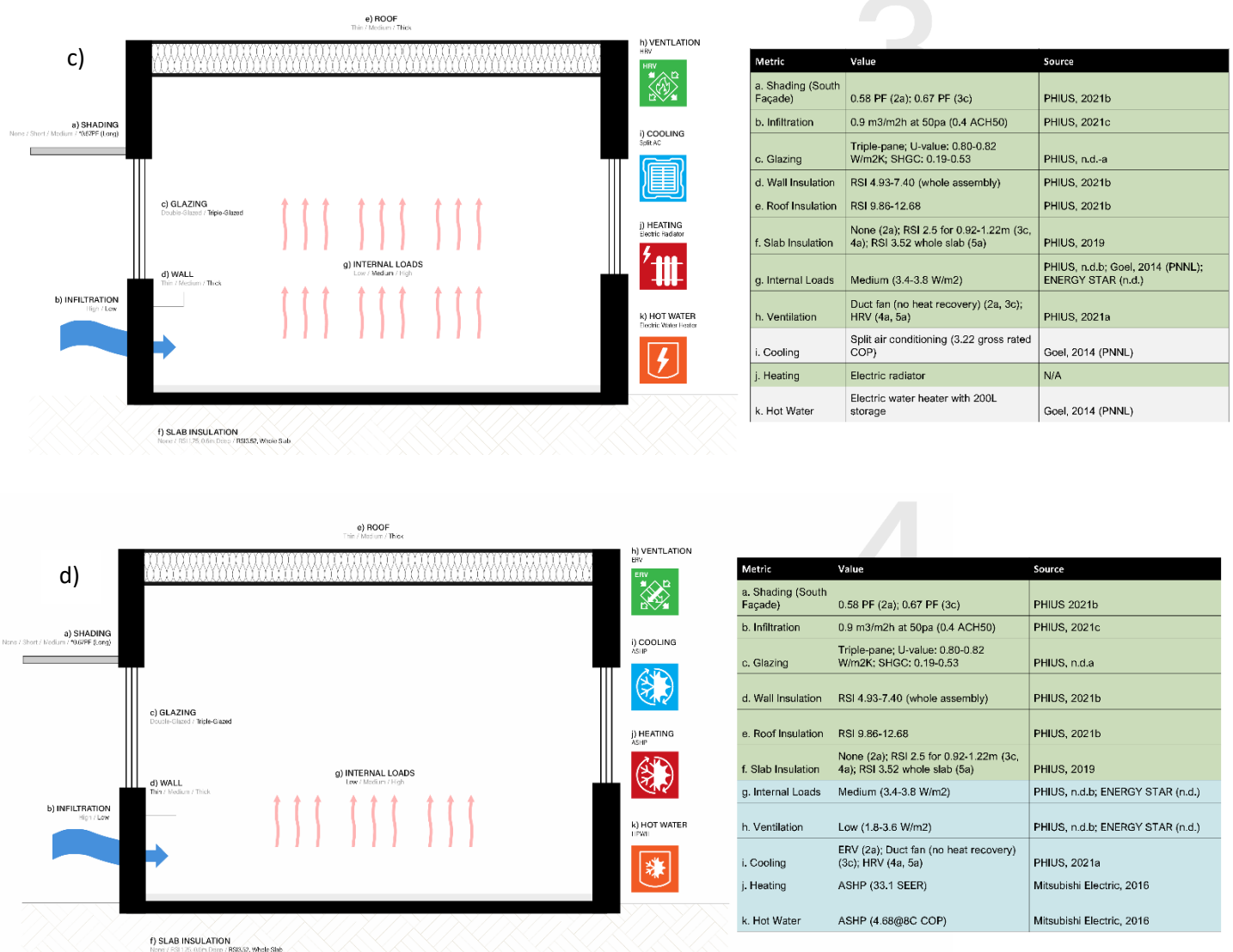


Figure 4: Diagrams of four principal energy simulation cases: a) Base case – ASHRAE 90.1-2004 b) Regenerative Mode – Code envelope with PHIUS equipment c) Conservative Mode – PHIUS envelope with code equipment d) Combined – PHIUS envelope and equipment. All diagrams were laid out by Adam Yarnell and executed by Bianca Seong.

Operational energy use was simulated in the Fraunhofer IBP's WUFI Plus platform (*WUFI Plus*, n.d.), which was selected specifically for its integrated passive house verification scope. The base building's geometry was transferred to SketchUp Pro 2021 (*SketchUp Pro 2021*, 2021) from the PNNL's ASHRAE901_ApartmentMidRise_STD2004_NewYork.idf file (Goel et al., 2014), which had been upgraded to EnergyPlus v9.6 with the IDFVersionUpdater utility in EP-Launch (*EP-Launch*, 2020). For the base cases (Fig. 4a), properties were taken directly from each climate zone's published IDF wherever

possible. Remaining simulation parameters were determined by consulting the ASHRAE 90.1-04 standard, searching through the BIRDS technical manual, and reviewing published literature.

The Regenerative Mode cases (*Fig. 4b*) were built to meet PHIUS 2021 targets with as few changes to the base envelopes as possible. Thermally-broken triple-pane windows and slab edge insulation in climate zones 4 and 5 were added to satisfy mandatory design requirements. Comparatively poor-performing glazing was selected from the PHIUS Certified Window Database based on products whose whole-assembly u-value and solar heat gain coefficient (SHGC) did not match PHIUS recommendations (PHIUS, n.d.-a). The extremely airtight envelope required by PHIUS—equivalent to 0.4 ACH50 (0.9 m³/m²h or 0.05 cfm/ft² envelope at 50pa)—is assumed, however, to have been achieved through careful detailing and without additional material inputs. Instead, high-efficiency HVAC equipment and appliances (*Tbl. 10b in Appx. C*), and correspondingly small internal loads (PHIUS, n.d.b), were used to lower heating and cooling demands and loads. The remaining energy reductions were achieved with minor wall and roof upgrades to ASHRAE 90.1-2019 for climates 2a and 4a, minimal southern shading for 2a (0.88m or a 0.42 projection factor, the minimum value recommended in the PHIUS CORE Prescriptive 2021 reference tables) (PHIUS, 2021b), and an additional 25cm (0.7 RSI) of slab insulation for 4a.

The Conservative Mode cases (*Fig. 4c*) were essentially an inversion of the Regenerative Mode cases where PHIUS 2021 targets were achieved using an overbuilt envelope and underperforming mechanical equipment. Insulation, glazing, and shading properties were all lifted directly from PHIUS prescriptive compliance recommendations (PHIUS, 2021b) (PHIUS, 2019) (PHIUS, n.d.-a). In line with PHIUS ventilation requirements, dedicated outdoor air systems (DOAS) were added for all climates, but heat recovery was not needed in 2a or 3c, and ventilation fan power for these climates was adjusted to the lowest value suggested by PHIUS. Likewise, in all climates, electric radiators replaced furnaces to maintain the space conditioning and ventilation separation. Finally, comparatively inefficient ENERGY STAR appliances (*Tbl. 10a in Appx. C*) and minimum-efficiency LED lighting (80% of fixtures meeting ENERGY STAR requirements) was specified to meet mandatory design requirements while still increasing internal loads. The final designs all met PHIUS heating and cooling demands and loads limits, but the source energy requirement proved impossible to meet without rooftop photovoltaics. PV, however, was excluded from this analysis to avoid data skewing from the outsized embodied footprint. A final combined case (*Fig. 4d*) paired the mechanical equipment of the Conservative Mode cases with the envelopes of the Regenerative Mode cases to simulate the highest performing buildings.

It should be noted that for both the Conservative Mode and Regenerative Mode cases the office in the Mid-rise Apartment prototype building was replaced with an additional dwelling unit due to constraints in modeling multiple typologies in the Passive House verification workflow of WUFI Plus. Lighting and miscellaneous electric loads, however, included the office as these figures were calculated outside WUFI Plus.

Table 5: Initial grid intensities of U.S.-Average and relevant eGRID subregions

Grid	Initial Carbon Intensity (kgCO2e/kWh)
U.S.-Average	0.3711701
FRCC (Tampa)	0.378785916
CAMX (San Diego)	0.232901538
NYCW (NYC)	0.287854254
NYUP (Buffalo)	0.105918354

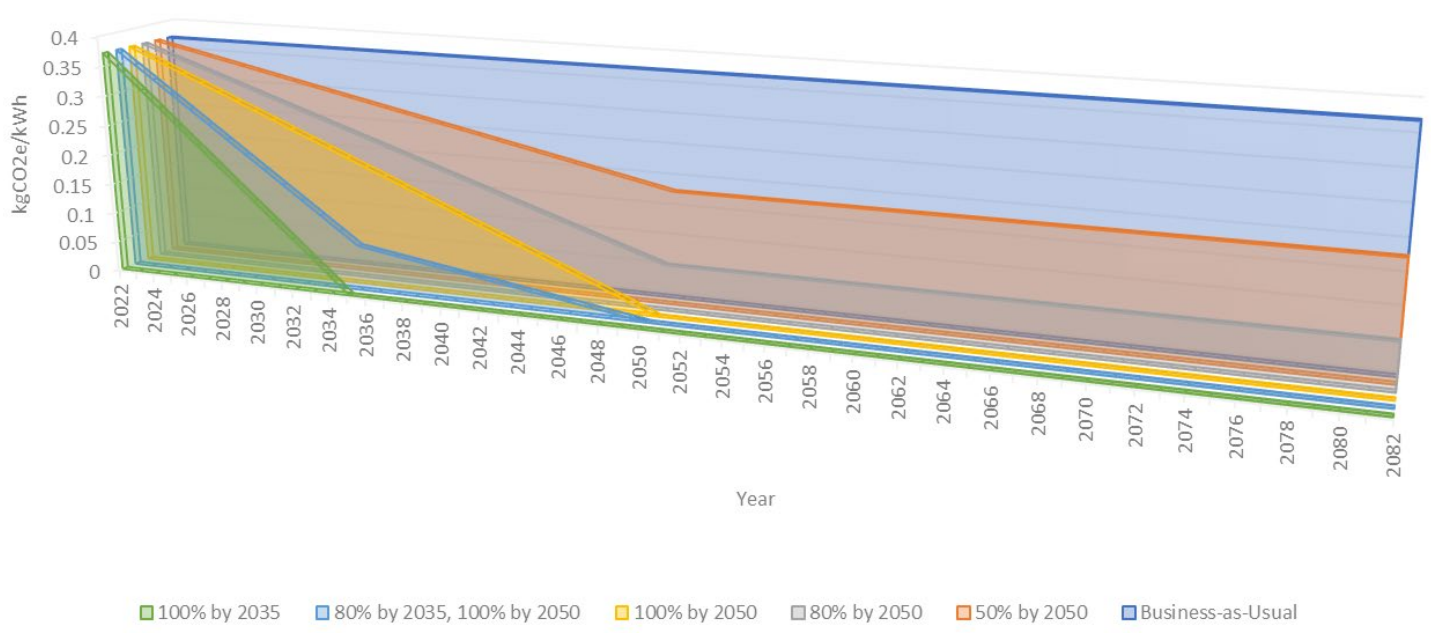


Figure 5: Cumulative emissions six decarbonization scenarios applied to the eGRID US-Average.

Ultimately, each case's annual site energy consumption was extracted from WUFI Plus and converted to carbon with modified grid emission factors from the EPA's eGRID tool (United States Environmental Protection Agency (EPA), 2022). The U.S. average grid emissions were used by default, but results were also computed where each reference city was assigned its eGRID subregion's initial grid intensity (*Tbl. 4*). Climate zone 3c, for instance, was assigned the CAMX subregion's initial grid intensity of 0.23 kgCO2e/kWh based on its reference city of San Diego. Linear decarbonization scenarios were then modeled from these initial grid intensities. Values were calculated annually from occupancy, 2022, through demolition, 2082, and the average intensity over these 60 years was then multiplied by the cumulative site energy use. *Fig. 5* shows the cumulative emissions for each scenario with an initial grid intensity set to the U.S. average. *Fig. 15* in *Appx. B* shows the annual grid intensities per scenario of each studied eGRID subregion.

b. Embodied Carbon

The buildings' embodied carbon was measured through whole-building life-cycle assessment (LCA). A modified system boundary adapted from EN 15804 (CEN, 2013) was used. The service life was set to 60 years to match (Stephan et al., 2013) and LEED BD+C v4 (U.S. Green Building Council, 2013), as well as other cases highlighted in (Grant & Ries, 2013). As follows, all building materials are assumed to enter end-of-life flows after 60 years. Stage A5 was excluded due to a lack of data; B6 was modeled separately in WUFI Plus; and B7, while important, falls outside narrow focus on carbon. Finally, as data quality for stage D is still very poor, its impacts were also excluded from the assessment.

Traditional Structure, foundation, enclosure, and interior partitions (SFEI) material inventories (<https://bit.ly/3MvRgxy>) were built for all cases with the EN 15978 (CEN, 2011) assessment tool in One Click LCA (*One Click LCA*, n.d.). Material composition and quantities for the base cases were extracted from two main PNNL resources (Goel et al., 2014): the prototype building scorecard (PNNL_Scorecard_Prototypes_Apartment_Midrise.xls) and published IDFs for each climate zone (e.g. ASHRAE901_ApartmentMidRise_STD2004_Tampa.idf). Additional details were provided by the BIRDS technical manual, and remaining assumptions were set in consultation with peer-reviewed literature, published technical guidance, manufacturer disclosures, and One Click LCA guidance. The Passive House material inventories used the base case inventories but substituted triple-pane windows and added additional wall, roof, and foundation insulation as needed. Finally, key materials were replaced with lower-carbon alternatives to create low-embodied-carbon cases for both code and Passive House buildings. The most impactful substitutions include mass timber for steel for columns and beams, biobased for petroleum-based for insulation, and blast-furnace slag and fly ash for Portland cement for foundations. Finally, biogenic carbon is tallied separately from all other flows. When biogenic carbon is included, a floor of zero is employed—as per EN 15804:2012+A1:2013 (CEN, 2013)—so that no building product is considered carbon-negative.



Figure 6: LCA data quality. Percentages are based on the number of components with individual data sources across all eight cases.

Material inventories for MEP equipment—including HVAC, domestic hot water, electric services, plumbing services, and appliances—for all cases were also built in One Click LCA (<https://bit.ly/3MvRgxy>). Data collection relied on the same sources used for the structure, foundation, enclosure, and interior partitions inventories. Components with poor data availability or quality,

however, were modeled in SimaPro (*SimaPro*, n.d.) using the Ecoinvent 3 database (Wernet et al., 2016) and TRACI 2.1 (Bare, 2011) characterization factors with US-2008 weighting. Specifically, inventories for gas furnaces, electric furnaces, and air-source heat pumps were sourced from the BIRDS technical manual, while an inventory for tankless water heaters was sourced from (Piroozfar et al., 2016). It should be noted that all space conditioning equipment was sized by heating and/or cooling capacity. Average peak loads per dwelling unit were calculated from the published ENERGY PLUS output reports for each climate zone (e.g. ASHRAE901_ApartmentMidRise_STD2004_Buffalo.table.htm). The peak loads calculated in WUFI Plus—again, averaged per dwelling unit—were then used to scale down the capacities for Passive House cases. All heating and cooling loads were then scaled up by 1.25 and 1.15, respectively, as per ASHRAE 90.1 recommendation (ANSI/ASHRAE/IES, 2004) (ANSI/ASHRAE/IES, 2019). Finally, these loads were matched to available models and capacities of the Mitsubishi Electric M-Series (Mitsubishi Electric, 2016). To avoid double counting, refrigerants were excluded from the life-cycle inventories of all HVAC equipment. Data quality statistics for both the SFEI and MEP inventories are presented in *Fig. 6*.

c. Refrigerants

Finally, a separate analysis was conducted to determine HVAC-related refrigerant impacts. The refrigerant charges of three representative pieces of equipment—an air source heat pump (ASHP), a heat pump water heater (HPWH), and split air conditioning (AC) system—were extracted and reduced down to an appropriate functional unit; one kW capacity was selected for air-source heat pump and split AC systems, while one unit was used for the heat pump water heater as the models available were already significantly oversized. Feasible lower and higher global warming potential alternatives were investigated (*Tbl. 7 in Appx. A*), and annual leakage and end-of-life loss scenarios were sourced from (George et al., 2019); these numbers were scaled up for the split AC based on information from Tabelle 50 of the ÖKOBAUDAT database (Bundesministerium für Wohnen, Stadtentwicklung und Bauwesen, 2021). Manufacturing emissions were averaged from the three available refrigerants (R404a, R407c, R410a) on ÖKOBAUDAT and scaled to the functional units. Note that the mass and operational performance of refrigerants were held constant, and all refrigerants are assumed to be recharged annual back to their original mass. A detailed calculation is found below in *Eq. 2*.

$$RI = kg_{refrig} * [kgCO2e_{mfr} + (GWP * AL * SL_{equip}) + (GWP * EOL)] * [SL_{equip} / SL_k] \quad (2)$$

Where, RI: Refrigerant impact (kgCO2e)

Kg_{refrig} : Total mass of initial refrigerant charge

$KgCO2e_{mfr}$: Embodied carbon of manufacturing (A1-A3)

GWP: 100-year Global Warming Potential of specified refrigerant

AL: Annual leakage (%)

EOL: End-of-life losses (%)

SL_{equip} : Service life of equipment (yrs)

SL_k : Service life of building (yrs)

Refrigerant charges and resulting refrigerant impacts are calculated for both oversized and rightsized equipment; the former keeps the ASHRAE 90.1 scaling factors while the latter is sized exactly to the calculated peak loads.

d. Summary



Figure 7: Key inherited changes in constructing code cases (above) and Passive House cases (below).

Table 6: List of five data filters and available options that can be used to generate 192 different life-cycle carbon comparison charts.

Data Filter	Option	Explanation
Grid	US Average	All climate zones initialized at 2020 US average: 0.37 kg/kWh (0.82 lb/kWh)
	eGrid Subregions	2a initialized at 2020 FRCC, 3c at 2020 CAMX (WECC California), 4a at 2020 NYCW (NPCC NYC/Westchester), 5a at 2020 NYUP (NPCC Upstate NY)
Decarbonization Scenario	Business-as-Usual	2020 grid intensity is held constant through 2022-2082
	50% by 2050	Grid intensity decreases linearly to 50% of 2020 rate 2022-2050, held constant 2050-2082
	80% by 2050	Grid intensity decreases linearly to 20% of 2020 rate 2022-2050, held constant 2050-2083

	100% by 2050	Grid intensity decreases linearly from 2020 rate in 2022 to 0 in 2050
	80% by 2035, 100% by 2050	Grid intensity decreases linearly to 20% of 2020 rate 2022-2035, decreases linearly from 20% to 0 2035-2050
	100% by 2035	Grid intensity decreases linearly from 2020 rate in 2022 to 0 in 2035
Biogenic Carbon	Exclude	Biogenic carbon storage is excluded from analysis
	Include	Biogenic carbon storage is subtracted from modules A-C totals, with a minimum value of 0 per material (EN 15804+A1)
Refrigerants	Baseline	R410a (ASHP and Split AC) and R134a (HPWH); 3.8% annual leakage and 2% EOL losses for heat pumps, 7.6% annual leakage and 2.78% EOL losses for split AC
	High	R404a (3921.6 GWP) for ASHP and split AC, R410a (2087.5 GWP) for HPWH; 6% annual leakage and 10% EOL losses for heat pumps 12% annual leakage and 13.92% EOL losses for split AC
	Lower	R32 (675 GWP) for ASHP and Split AC, R513a (629.76 GWP) for HPWH; 3.8% annual leakage and 2% EOL losses for heat pumps, 7.6% annual leakage and 2.78% EOL losses for split AC
	Lowest	R1234ze (1 GWP) for ASHP and Split AC, R744 (1 GWP) for HPWH; 1% annual leakage and 1% EOL losses for heat pumps, 2% annual leakage and 1.39% EOL losses for split AC
HVAC Sizing	Oversized	Heating and cooling capacities set at 125% and 115% of peak loads as per ASHRAE 90.1 (refrigerants only)
	Rightsized	Heating and cooling capacities set at 100% of peak loads (refrigerants only)

Eight final cases are presented above in *Fig. 7*: four code cases and four PHIUS cases. Key transformations are also shown in *Fig. 16* in Appx. C. The results of all three assessments for each climate zone of these eight cases are summed and presented in a Microsoft Excel pivot table published to Github (<https://bit.ly/3MvRgXv>). Users can select two different grid specificities, six different decarbonization scenarios, two treatments of biogenic carbon, four refrigerant impact scenarios, and two HVAC sizing scenarios (*Tbl. 6*)

IV. Results

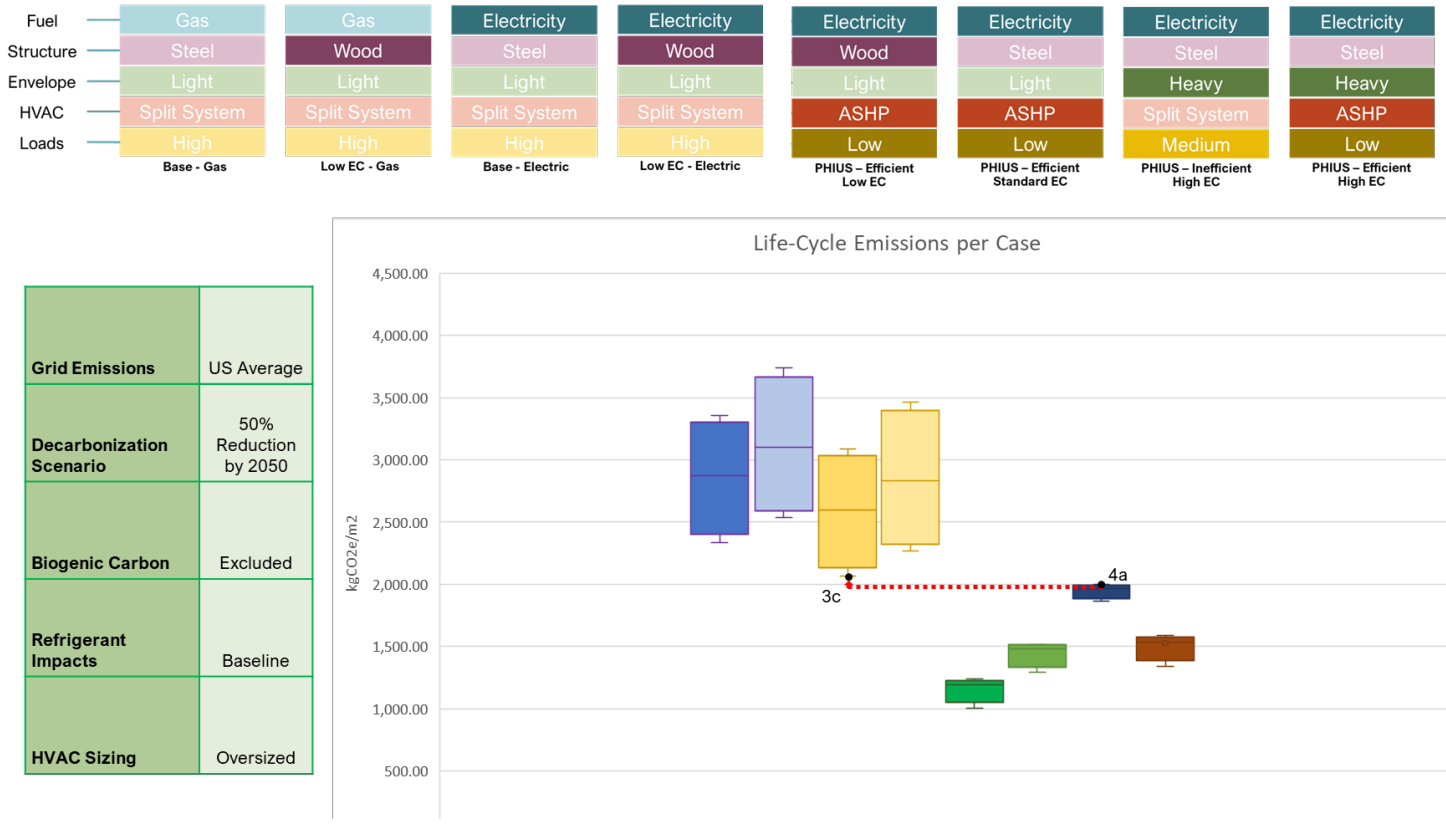


Figure 8: Box and whiskers plot of the reference scenario. The table on the left lists the selected data filters, and the legend above shows the most important attributes of each case.

As noted in the introduction, the analysis produced a total of 6144 building iterations, and it is therefore imprudent to discuss all results in detail. First, a reference scenario should be established with baseline values for all five data filters: “US-Average” for grid emissions, “50% Reduction by 2050” for decarbonization scenario, “Excluded” for biogenic carbon, “Baseline” for refrigerant impacts, and “Oversized” for HVAC sizing. Reviewing a box and whiskers plot of this reference scenario (Fig. 8), where the whiskers represent the minimum and maximum emitting climate zones for each case, reveals considerably more variability in the code cases on the left than the Passive House cases on the right. These distributions also highlight the importance of climate, as code buildings in mild climates (San Diego, 3c) perform nearly as well as some passive house buildings in harsher climates (New York City, 4a).

The Evolving Carbon Balance of High-Performance Buildings

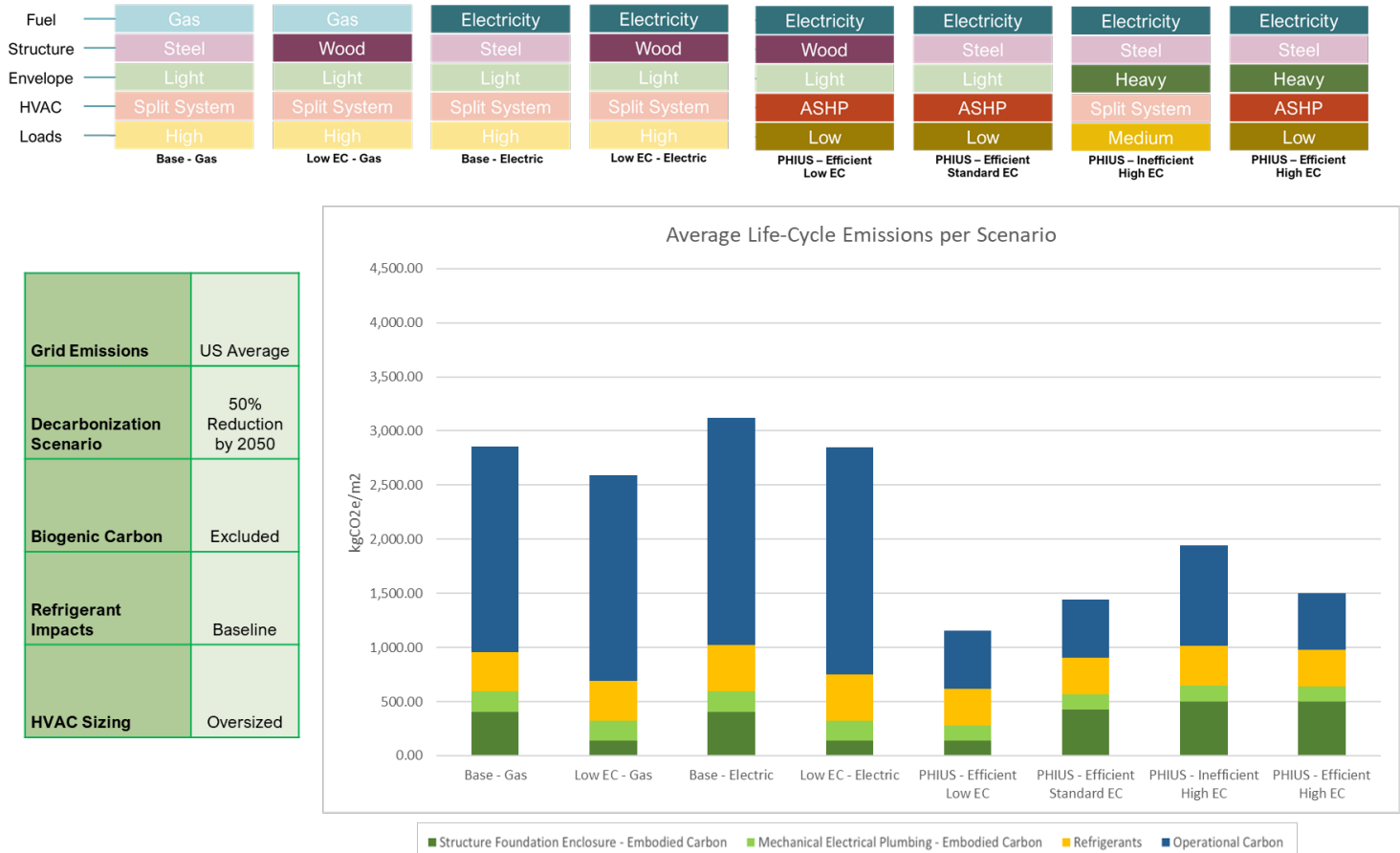


Figure 9: Average life-cycle emissions for the eight case (four code, four Passive House) using the reference scenario data filters.

Reviewing average life-cycle emissions per case—where the mean value for each building domain (SFEI embodied carbon, MEP embodied carbon, refrigerant carbon, and operational carbon) is used—offers more useful insights. Fig. 9 presents the average life-cycle emissions for the reference scenario. SFEI embodied carbon constitutes an average of 15% of life-cycle carbon for all cases, MEP embodied carbon makes up 7%, refrigerant carbon totals 17%, and operational carbon comprises an average 60% of total life-cycle carbon; if focus is pulled to just the code cases, operational carbon increases to 70% of emissions, consistent with literature.

The Evolving Carbon Balance of High-Performance Buildings



Figure 10: Reference scenario comparison of the lowest-emitting code case and highest-emitting Passive House case using initial grid intensities set to a) the U.S. average and b) specific regional grids.

The Evolving Carbon Balance of High-Performance Buildings



Figure 11: Comparison of gas and electric cases with a) a high-carbon electric grid and b) a rapidly decarbonized grid.

Results are highly sensitive to electricity grid assumptions. For example, if a scenario with low embodied impacts (biogenic carbon included, lower refrigerant impacts, and rightsized equipment) is entered, switching from the best-performing code case to the worst-performing Passive House case reduces emissions by 21% (*Fig. 10a*). When grid emissions are set to local grids (eGRID subregions), however, the difference between the above-mentioned cases virtually disappears. The Passive House case will emit just 5% less carbon than the code case, easily within an assumed margin of error (*Fig. 10b*).

The rate of electric grid decarbonization is the key determinant of life cycle emissions for the code cases. If the reference scenario switches to a business-as-usual decarbonization, the gas furnace cases (“Base – Gas” and “Low EC – Gas”) emit 19-20% less than the electric furnace cases (“Base – Electric” and “Low EC – Electric”) over their lifetimes (*Fig. 11a*). If grid emissions fall by 80% by 2050, the electric cases release 3-4% less life-cycle carbon than the gas cases. In the steepest decarbonization scenario, selecting an electric furnace over a gas furnace reduces total carbon dioxide emissions by 26-30% (*Fig. 11b*).

The Evolving Carbon Balance of High-Performance Buildings

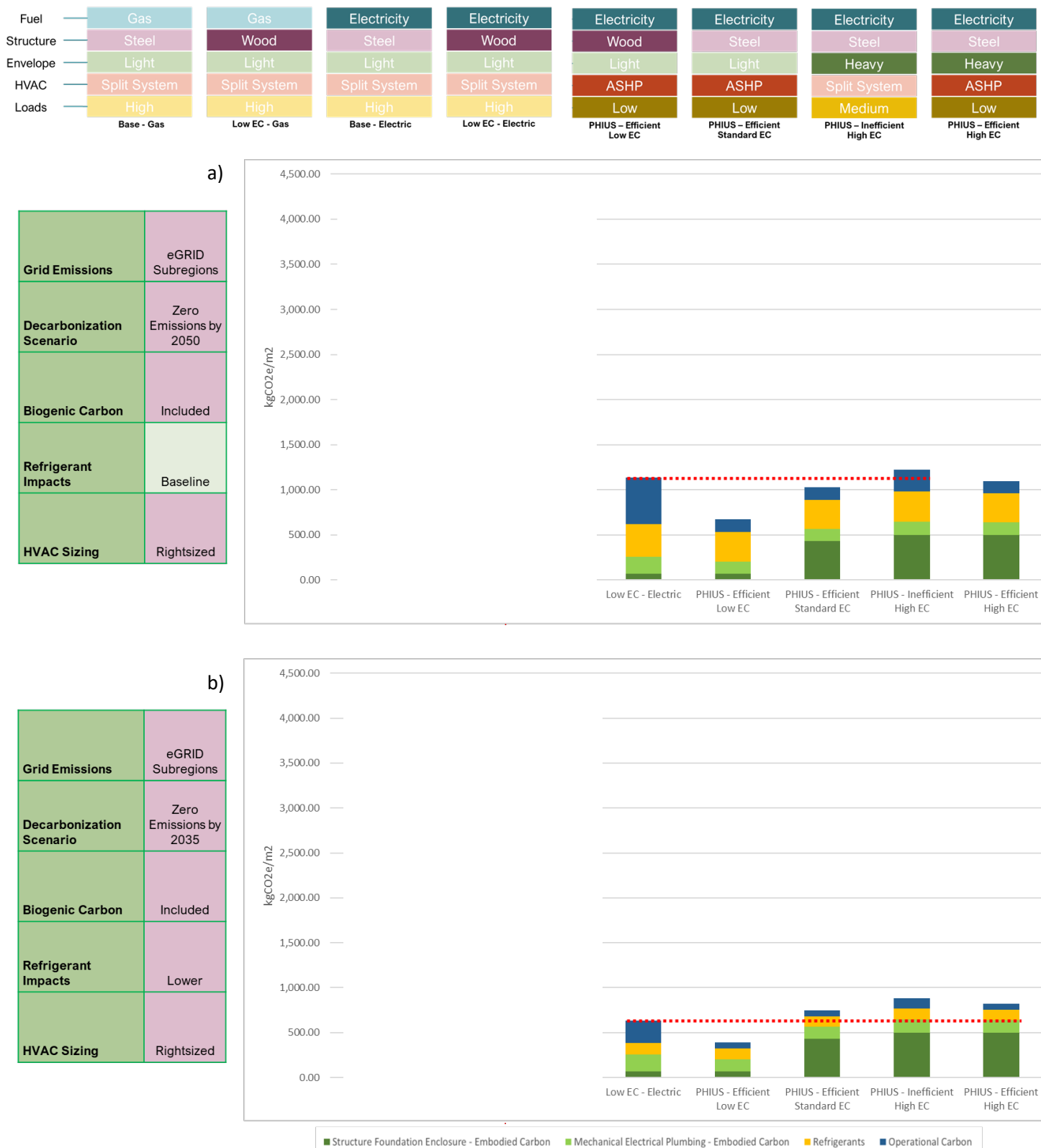


Figure 12: Comparison of a low-embodied-carbon code case with Passive House cases in a) moderate and b) idealized scenarios.

Significantly, this low-embodied-carbon code case outperforms Passive House cases when the electricity grid is decarbonized with sufficient rapidity. Using eGRID subregions and assuming zero electricity emissions by 2050 with baseline refrigerant impacts, the all-electric code case with low-embodied-carbon materials (“Low EC – Electric”) emits less carbon dioxide over its lifetime than the Conservative Mode Passive House case with standard-embodied-carbon materials (“PHIUS – Inefficient High EC”) in three scenarios: excluded biogenic carbon and rightsized HVAC (1.7% less), included biogenic carbon and oversized HVAC (4.8% less), and included biogenic carbon and rightsized HVAC (7.4% less) (*Fig. 12a*). In a zero-carbon-by-2035 scenario, the code case also emits 4.3% less than the combined Regenerative-Conservative Mode case (PHIUS – Efficient High EC) with excluded biogenic carbon, baseline refrigerant impacts, and oversized HVAC. If biogenic carbon is included or refrigerant impacts are lowered or HVAC equipment is rightsized, the low-embodied-carbon code case emits less than three of four Passive House cases. And if all ideal conditions are met—including biogenic carbon and lower refrigerant impacts and rightsized HVAC—the “Low EC Electric” case emits 15.7%, 22.9%, and 28.2% less than the “PHIUS – Efficient Standard EC”, “PHIUS – Efficient High EC”, and “PHIUS Inefficient High EC” cases, respectively (*Fig. 12b*).

Life-cycle emissions also show significant sensitivity to SFEI material choice. In the reference scenario (*Fig. 9*), substitution of low-embodied-carbon assemblies for high-embodied-carbon assemblies reduces SFEI carbon by 66.5%. These lower SFEI impacts reduce total emissions by 11.1%, a figure which rises to 20.0% when only the operationally-identical Passive House cases (“PHIUS – Efficient Low EC” and “PHIUS – Efficient Standard EC”) are considered. Examining the life-cycle inventory for the Buffalo climate of the base case reveals the most impactful substitutions. Replacing steel with wood—glue-laminated timber for steel columns and beams, cross-laminated timber for steel decking and concrete floor slabs, wood framing for steel framing—reduces SFEI emissions by 50%; replacing mineral-based insulations with biobased insulations—cellulose fiberboard for extruded polystyrene and polyisocyanurate, blown-in cellulose for fiberglass—reduces SFEI emissions by 6%; and replacing Portland cement with supplementary cementitious materials—50% fly ash or ground-granulated blast-furnace slag cement concrete mixes for 100% Portland cement concrete mixes—reduces SFEI emissions by 1%.

The Evolving Carbon Balance of High-Performance Buildings

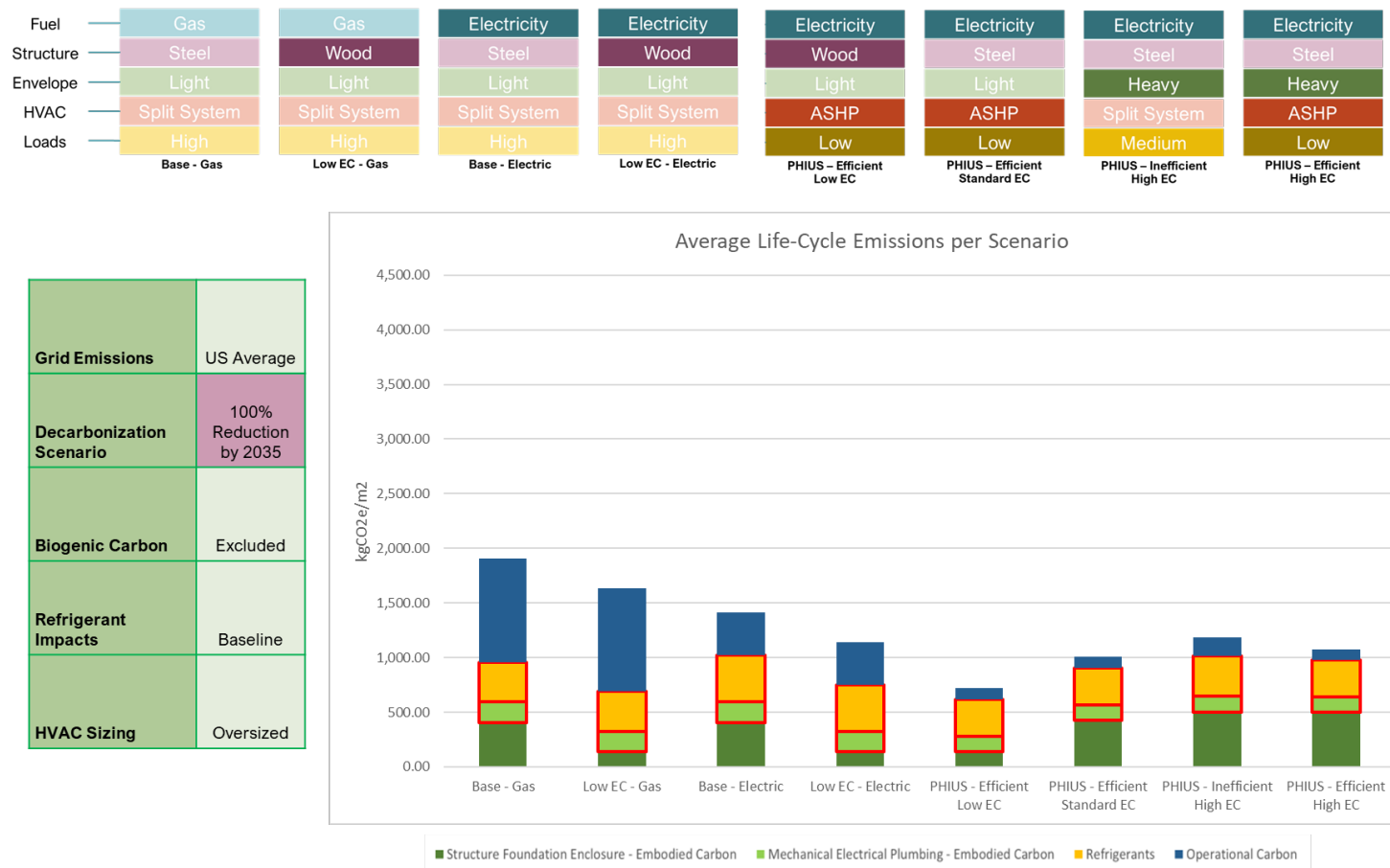


Figure 13: Relative contribution of MEP equipment (embodied carbon and refrigerants) to life-cycle emissions in a rapidly-decarbonized scenario.

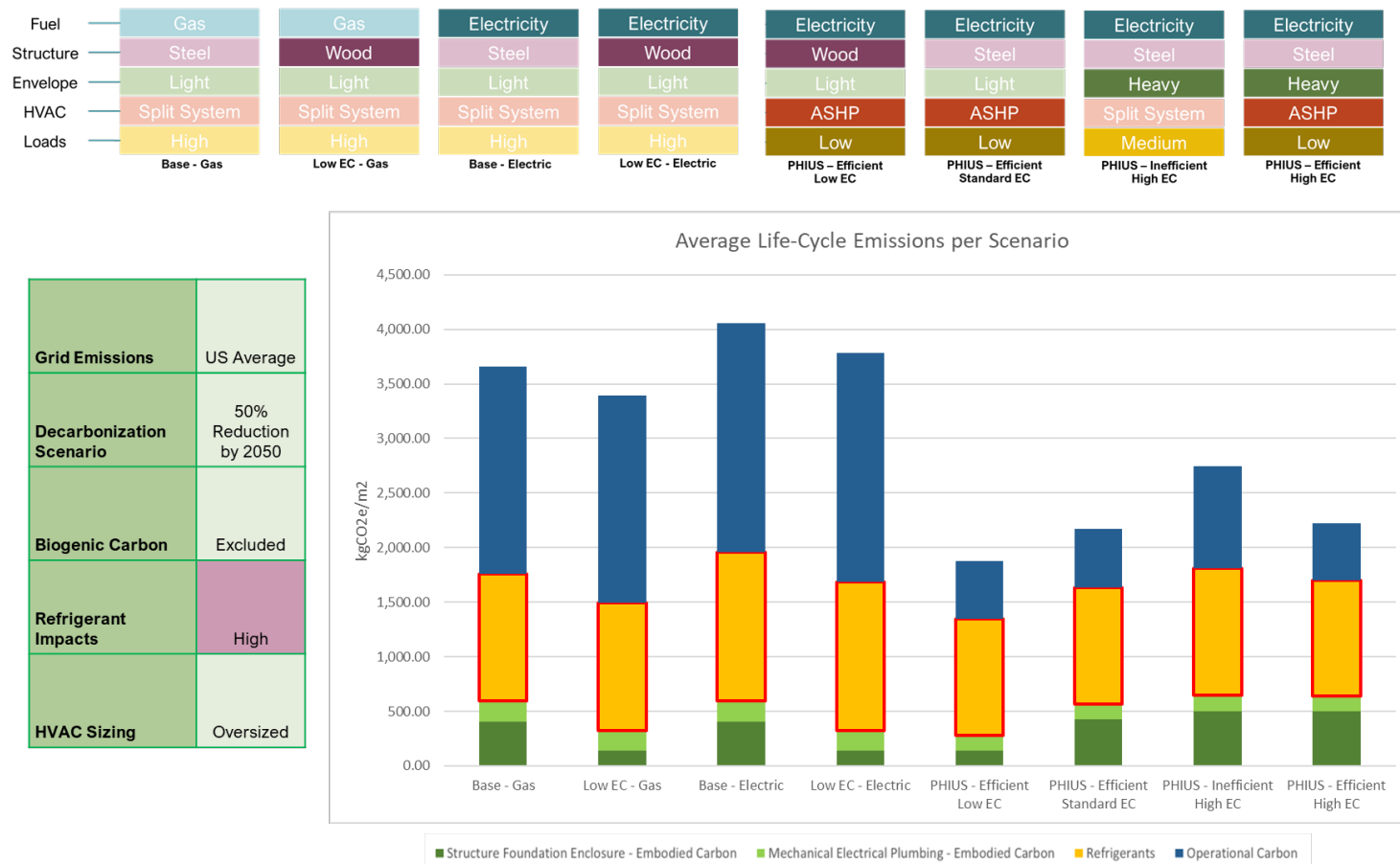


Figure 14: Relative contribution of refrigerants to life-cycle emissions in a high impact scenario.

In nearly all iterations, MEP equipment (embodied carbon and refrigerant impacts) constitutes a significant portion of total life-cycle emissions. The average of 24% in the reference scenario is higher than most sources in the literature, but this figure is driven principally by refrigerants (17% of total life-cycle emissions); the 7% figure just for MEP equipment is in line with or even below the literature, which mostly excludes refrigerants. The relative contribution of MEP equipment rises precipitously the more rapidly the electric grid decarbonizes. In a net-zero-by-2050 scenario, 36% of life-cycle emissions are tied to MEP embodied carbon and refrigerant impact, and this proportion exceeds 42% in a net-zero-by-2035 scenario (Fig. 13).

The refrigerant impacts themselves are also extremely sensitive to their underlying assumptions. In the lowest scenario, where refrigerant impacts are held at 1 GWP and leakage and EOL losses are minimized, refrigerants constitute an average of 0.01% of life-cycle carbon. Selecting a lower refrigerant impact—630-675 GWP, 1-2% annual leakage rate, and 1-1.4% EOL losses—raises the average refrigerant carbon contribution to 7% of building's total life-cycle emissions. In the very worst refrigerant scenario—2088-3922 GWP, 6-12% annual leakage rate, and 10-13.9% EOL losses—refrigerants constitute just under 40% of average impacts across all cases and nearly 50% for the Passive House cases (Fig. 14).

V. Discussion

Many experimental constraints have already been discussed in the Methodology section, but it is important to highlight a few key limitations that provide important context to this research.

- ASHRAE 90.1-2004 may not reflect standard practice for new construction. ASHRAE 90.1-2013, in turn, is adopted in a plurality of states (U.S. Department of Energy, Building Technologies Office, 2022), and the standard aligns with buildings that consume 15% less site energy (Halverson, Liu, et al., 2010; Halverson, Williamson, et al., 2010; Halverson et al., 2014). Projects built to 90.1-13 or 90.1-19 will tend to match Passive House emissions at more moderate grid decarbonization scenarios, but the more massive envelopes required by these standards may reduce life-cycle benefits in rapid decarbonization scenarios. Further simulation is needed.
- There may have been a loss of fidelity in adapting commercial building prototypes from EnergyPlus to WUFI Plus. The two platforms, for instance, require different approaches for modeling glazing, infiltration, and thermal bridging. Furthermore, internal mass was held constant between cases, and, despite simulating Passive Houses, thermal bridging was only explored at a limited resolution (duct penetrations for DOAS). It is likely worthwhile in the future to build out all operational cases in EnergyPlus and compare the results to the WUFI Plus simulations.
- The refrigerant impact analysis may not accurately represent real-world performance. As noted previously, the leakage rates assume annual recharge and likely overestimate impacts. Likewise, refrigerant parameters and operational energy are held constant, despite research pointing to small but appreciable changes to charge, capacity, and efficiency resulting from refrigerant substitutions (Goetzler et al., 2016). Future work would also benefit from modeling alternative systems like variable refrigerant flow (VRF) HVAC with higher refrigerant charges and greater variation in installed capacity; expanding reference cities to more extreme climate may also add refrigerant charge variation. Finally, although it is beyond the scope of this thesis, building a fully passive case without any HVAC equipment in a suitable climate would offer a compelling counterexample to eight presented cases.
- Linear decarbonization does not reflect predicted grid emissions. The NYCW subregional grid, for instance, is expected to increase in emissions intensity in the near-term (Vahidi et al., 2021). Future scenarios should be built with published data from the U.S. Energy Information Agency (EIA) and decarbonization pathways from Intergovernmental Panel on Climate Change (IPCC) reports. Future work may also benefit from exploring upstream embodied impacts from rapid electrification.
- Finally, the LCA results are highly sensitive to their data source. Although a structured sensitivity analysis was not undertaken in this study, one should acknowledge that the data quality of Environmental Product Declarations (EPD) and other sources used in whole-building LCAs varies widely (Waldman et al., 2020). Future work could also explore building service life sensitivity and the effect of changing electricity grid intensities on manufacturing emissions.

VI. Conclusions

This thesis seeks to explore the whole-life-carbon implications of low-energy building designs. A representative case study is established, and the three linked assessments used to calculate life-cycle carbon (operational energy simulation, life-cycle assessment, and refrigerant impact analysis) are described in detail. The results, summarized in the previous section, reveal six principal conclusions.

- Life-cycle carbon emissions are highly dependent on future energy grid intensity and building constructions. Therefore, optimal designs can vary significantly for cities with identical climates but divergent grid emissions.
- As the rate of grid decarbonization increases, embodied carbon will constitute a greater proportion of total life-cycle emissions, and greater effort should be made to reduce embodied carbon. Especially in scenarios with steep grid decarbonization, the overbuilt envelopes of Conservative Mode architecture lose their emissions justification, and operationally inefficient buildings with less carbon-intensive materials and equipment prevail over high-performance buildings with standard materials and equipment. A rush to build less massive buildings should be tempered by a high degree of caution, however, as this finding only applies to locations that have already made significant strides to fight climate change.
- Building electrification without rapid energy grid decarbonization may not reduce total life-cycle emissions. In the code cases, electric furnaces did not begin to outperform gas furnaces until electricity emissions were cut by 80% over 28 years. One suspects that case studies that focused on colder climates or used base buildings with gas water heaters would need an even more aggressive inflection point.
- Material substitution with low-embodied alternatives can effect considerable overall carbon reduction, especially as operational performance improves and the grid decarbonizes. Even in the very worst case—U.S. average grid, business-as-usual emissions, biogenic carbon excluded, high refrigerant impacts, and oversized equipment—thoughtful material specification still reduces life-cycle carbon by 6% in the code cases. Assuming the substitution of equally- or at least comparably-performing materials, it always appears worthwhile to designate low-carbon SFEI materials.
- Embodied emissions from building MEP services constitute, at present, a significant portion of life-cycle carbon emissions, and cleaner energy grids will increase services' relative share of carbon. Contemporary LCAs limited to SFEI, therefore, tend to under-report carbon emissions. Inclusion of MEP and refrigerant impacts in future studies will facilitate more informed decision-making.
- Overall life-cycle emissions are strongly driven by both the choice of refrigerants and the diligence of maintenance and replacement over the entire estimated service life of the building. The use of high-GWP refrigerants in high-performance buildings can negate much of the life-cycle benefit of reduced operational emissions. More importantly, many suitable low-GWP refrigerants are already on the market, and this case study suggests using the alternatives will effect an appreciable emissions reduction.

Finally, in all scenarios, the “PHIUS – Efficient Low EC” case is associated with the lowest life-cycle carbon emissions. This result steers a designer toward Regenerative Mode architecture with low-

embodied-carbon materials, but they should proceed cautiously until results can be compared with low-embodied carbon Conservative Mode cases in future studies.

VII. References

- Abergel, T., Dean, B., & Dulac, J. (2017). *Global Status Report 2017: Towards a zero-emission, efficient, and resilient buildings and construction sector*. UN Environment and International Energy Agency.
- Agrodomo. (2016). *Environmental Product Declaration of Accoya frames, turn, turn and tilt for NBvT [Environmental Product Declaration]*. Cycle Assessment Procedure for Eco-Impacts of Materials (CAPEM), Nederlandse Branchevereniging voor de Timmerindustrie (NBvT). <https://www.accoya.com/app/uploads/2020/05/Environmental-Product-Declaration-%E2%80%93-window-frames-%E2%80%93-EN-15804.pdf>
- Akbarnezhad, A., & Xiao, J. (2017). Estimation and Minimization of Embodied Carbon of Buildings: A Review. *Buildings*, 7(1), 5. <https://doi.org/10.3390/buildings7010005>
- ANSI/ASHRAE/IES. (2004). *ANSI/ASHRAE/IES Standard 90.1-2004: Energy Standard for Buildings Except Low-Rise Residential Buildings*. American Society of Heating, Refrigerating and Air-Conditioning Engineers.
- ANSI/ASHRAE/IES. (2019). *ANSI/ASHRAE/IES Standard 90.1-2019: Energy Standard for Buildings Except Low-Rise Residential Buildings*. American Society of Heating, Refrigerating and Air-Conditioning Engineers.
- Athalye, R., Halverson, M., Rosenberg, M., Liu, B., Zhang, J., Hart, R., Mendon, V., Goel, S., Chen, Y., Xie, Y., & Zhao, M. (2017). *Energy Savings Analysis: ANSI/ASHRAE/IES Standard 90.1-2016 (DOE/EE-1614)*. Pacific Northwest National Lab. (PNNL), Richland, WA (United States). <https://doi.org/10.2172/1764647>
- Azari, R., & Abbasabadi, N. (2018). Embodied energy of buildings: A review of data, methods, challenges, and research trends. *Energy and Buildings*, 168, 225–235. <https://doi.org/10.1016/j.enbuild.2018.03.003>
- Banham, R. (1984). *Architecture of the Well-Tempered Environment*. University of Chicago Press.
- Bare, J. (2011). TRACI 2.0: The tool for the reduction and assessment of chemical and other environmental impacts 2.0. *Clean Technologies and Environmental Policy*, 13(5), 687–696. <https://doi.org/10.1007/s10098-010-0338-9>
- Beshr, M., Aute, V., Abdelaziz, O., Fricke, B., & Radermacher, R. (2017). Potential emission savings from refrigeration and air conditioning systems by using low GWP refrigerants. *The International Journal of Life Cycle Assessment*, 22(5), 675–682. <https://doi.org/10.1007/s11367-016-1186-6>
- Bundesministerium für Wohnen, Stadtentwicklung und Bauwesen. (2021). *ÖKOBAUDAT version 2021-II: ÖKOBAUDAT according to EN 15804+A1*. Bundesministerium für Wohnen, Stadtentwicklung und Bauwesen. https://www.oekobaudat.de/no_cache/en/database/search/daten/db1.html#bereich1

- CEN. (2011). *BS EN 15978:2011 Sustainability of Construction Works—Assessment of Environmental Performance of Buildings—Calculation Method*. CEN.
- CEN. (2013). *BS EN 15804:2012+A1:2013 Sustainability of construction works—Environmental product declarations—Core rules for the product category of construction products*. CEN.
- Chastas, P., Theodosiou, T., & Bikas, D. (2016). Embodied energy in residential buildings—towards the nearly zero energy building: A literature review. *Building and Environment*, 105, 267–282. <https://doi.org/10.1016/j.buildenv.2016.05.040>
- Cole, R. J., & Kernan, P. C. (1996). Life-cycle energy use in office buildings. *Building and Environment*, 31(4), 307–317. [https://doi.org/10.1016/0360-1323\(96\)00017-0](https://doi.org/10.1016/0360-1323(96)00017-0)
- Cole, R. J., & Rousseau, D. (1992). Environmental auditing for building construction: Energy and air pollution indices for building materials. *Building and Environment*, 27(1), 23–30. [https://doi.org/10.1016/0360-1323\(92\)90004-9](https://doi.org/10.1016/0360-1323(92)90004-9)
- Connaughton, J. N. (1987). The Energy Cost of Construction. In D. O. Pedersen & J. Lemessany (Eds.), *Building economics: CIB proceedings of the fourth international symposium on building economics*. Danish Building Research Institute.
- Copiello, S. (2017). Building energy efficiency: A research branch made of paradoxes. *Renewable and Sustainable Energy Reviews*, 69, 1064–1076. <https://doi.org/10.1016/j.rser.2016.09.094>
- D'Amico, B., & Pomponi, F. (2020). On mass quantities of gravity frames in building structures. *Journal of Building Engineering*, 31, 101426. <https://doi.org/10.1016/j.jobe.2020.101426>
- Dixit, M. K. (2019). Life cycle recurrent embodied energy calculation of buildings: A review. *Journal of Cleaner Production*, 209, 731–754. <https://doi.org/10.1016/j.jclepro.2018.10.230>
- EP-Launch* (2.14b). (2020). [Computer software]. GARD Analytics.
- Fay, R., Treloar, G., & Iyer-Raniga, U. (2000). Life-cycle energy analysis of buildings: A case study. *Building Research & Information*, 28(1), 31–41. <https://doi.org/10.1080/096132100369073>
- George, B., Clara, L. H., & Levey, R. (2019). Understanding the Importance of Whole Life Carbon in the Selection of Heat-Generation Equipment. *CIBSE Technical Symposium*, 55.
- Goel, S., Rosenberg, M., Athalye, R., Xie, Y., Wang, W., Hart, R., Zhang, J., & Mendon, V. (2014). *Enhancements to ASHRAE Standard 90.1 Prototype Building Models* (PNNL-23269). Pacific Northwest National Lab. (PNNL), Richland, WA (United States). <https://doi.org/10.2172/1764628>
- Goetzler, W., Guernsey, M., Young, J., Fujrman, J., & Abdelaziz, A. (2016). *The Future of Air Conditioning for Buildings*. U.S. Department of Energy, Office of Energy Efficiency & Renewable Energy, Building Technologies Office.

- Grant, A., & Ries, R. (2013). Impact of building service life models on life cycle assessment. *Building Research & Information*, 41(2), 168–186.
<https://doi.org/10.1080/09613218.2012.730735>
- GreenSpec. (2022). *Crosslam CLT: Roof construction examples*.
<http://www.greenspec.co.uk/building-design/crosslam-timber-roofing-examples/>
- Grinham, J., Fjeldheim, H., Yan, B., Helge, T. D., Edwards, K., Hegli, T., & Malkawi, A. (2022). Zero-carbon balance: The case of HouseZero. *Building and Environment*, 207, 108511.
<https://doi.org/10.1016/j.buildenv.2021.108511>
- GUTEX Holzfaserplattenwerk. (2021). *Product Applications: The best wood fibre insulation for roofs, walls and interiors*. GUTEX Holzfaserplattenwerk.
https://gutex.de/fileadmin/uploads/Downloads/Broschueren/GUTEX_Anwenderbroschuere_en.pdf
- Halverson, M. A., Hart, R., Athalye, R. A., Rosenberg, M. I., Richman, E. E., & Winiarski, D. W. (2014). *ANSI/ASHRAE/IES Standard 90.1-2013 Preliminary Determination: Qualitative Analysis* (PNNL-23198). Pacific Northwest National Lab. (PNNL), Richland, WA (United States). <https://doi.org/10.2172/1131375>
- Halverson, M. A., Liu, B., Richman, E. E., & Winiarski, D. W. (2010). *ANSI/ASHRAE/IESNA Standard 90.1-2007 Preliminary Qualitative Determination* (PNNL-19791). Pacific Northwest National Lab. (PNNL), Richland, WA (United States). <https://doi.org/10.2172/1033848>
- Halverson, M. A., Williamson, J. L., Liu, B., Rosenberg, M. I., & Richman, E. E. (2010). *ANSI/ASHRAE/IESNA Standard 90.1-2010 Preliminary Qualitative Determination* (PNNL-20458). Pacific Northwest National Lab. (PNNL), Richland, WA (United States).
<https://doi.org/10.2172/1025693>
- Hannon, B. M., Stein, R. G., Segal, B., Serber, D., & Stein, C. (1976). *Energy use for building construction. Final report, March 1, 1976—December 31, 1976* (COO-2791-3). Illinois Univ., Urbana (USA). Center for Advanced Computation; Stein (Richard G.) and Associates, Architects, New York (USA). <https://doi.org/10.2172/7301380>
- Hein, M., Jones, D. A., & Eckert, C. M. (2021). UNDERSTANDING THE EMBEDDED CARBON CHALLENGES OF BUILDING SERVICE SYSTEMS. *Proceedings of the Design Society*, 1, 3279–3288. <https://doi.org/10.1017/pds.2021.589>
- Hernandez, P., & Kenny, P. (2011). Development of a methodology for life cycle building energy ratings. *Energy Policy*, 39(6), 3779–3788. <https://doi.org/10.1016/j.enpol.2011.04.006>
- Ibn-Mohammed, T., Greenough, R., Taylor, S., Ozawa-Meida, L., & Acquaye, A. (2013). Operational vs. Embodied emissions in buildings—A review of current trends. *Energy and Buildings*, 66, 232–245. <https://doi.org/10.1016/j.enbuild.2013.07.026>
- Jin, L., Cao, F., Yang, D., & Wang, X. (2016). Performance investigations of an R404A air-source heat pump with an internal heat exchanger for residential heating in northern China.

International Journal of Refrigeration, 67, 239–248.
<https://doi.org/10.1016/j.ijrefrig.2016.03.004>

Kneifel, J., O'Rear, E., Webb, D., & O'Fallon, C. (2018). An exploration of the relationship between improvements in energy efficiency and life-cycle energy and carbon emissions using the BIRDS low-energy residential database. *Energy and Buildings*, 160, 19–33.
<https://doi.org/10.1016/j.enbuild.2017.11.030>

Livchak, D., Hedrick, R., Young, R., Finck, M., Bell, T., & Karsz, M. (2019). *Residential Cooktop Performance and Energy Comparison Study* (Frontier Energy Report # 501318071-R0). Frontier Energy.

Lstiburek, J. W. (2004). Understanding vapor barriers. *ASHRAE Journal*, 46, 40–47.

Mitsubishi Electric. (2016). *M-Series Efficiencies*.

Moore, A. D., Urmee, T., Bahri, P. A., Rezvani, S., & Baverstock, G. F. (2017). Life cycle assessment of domestic hot water systems in Australia. *Renewable Energy*, 103, 187–196.
<https://doi.org/10.1016/j.renene.2016.09.062>

One Click LCA. (2021). *Average Material Quantities*. One Click LCA Help Centre.
<https://oneclicklca.zendesk.com/hc/en-us/articles/360015033400-Average-Material-Quantities>

One Click LCA (0.3.2). (n.d.). [Computer software]. Bionova Ltd.

Pham, H., & Rajendran, R. (2012). R32 And HFOs As Low-GWP Refrigerants For Air Conditioning. *International Refrigeration and Air Conditioning Conference*.
<https://docs.lib.purdue.edu/iracc/1235>

Phillips, R., Troup, L., Fannon, D., & Eckelman, M. J. (2020). Triple bottom line sustainability assessment of window-to-wall ratio in US office buildings. *Building and Environment*, 182, 107057. <https://doi.org/10.1016/j.buildenv.2020.107057>

PHIUS. (n.d.-a). *PHIUS Verified Window Performance Data Program: Program Overview*. Passive House Institute US. http://www.phius.org/documents/2017-01-06_Program-Overview_PHIUS-Verified-Window-Performance-Data-Program.pdf

PHIUS. (2019). *PHIUS+ 2018 Certification Guidebook*, v2.0.

PHIUS. (2021a). *HVI Winter Ratings*.

PHIUS. (2021b). *PHIUS CORE Prescriptive 2021—Reference Tables*, v1.0.
<https://www.phius.org/phius-core-prescriptive-2021-climate-zone-table>

PHIUS. (2021c). *PHIUS 2021 Passive Building Standard Certification Guidebook*, V3.02.

PHIUS. (2021d). *Sanden CO2 calculator for PHIUS Certification*, v3.1.

PHIUS. (n.d.b). *PHIUS Multi-Family Calculator*, v4.2.

Piroozfar, P., Pomponi, F., & Farr, E. R. P. (2016). Life cycle assessment of domestic hot water systems: A comparative analysis. *International Journal of Construction Management*, 16(2), 109–125. <https://doi.org/10.1080/15623599.2016.1146111>

Pomponi, F., & Moncaster, A. (2016). Embodied carbon mitigation and reduction in the built environment – What does the evidence say? *Journal of Environmental Management*, 181, 687–700. <https://doi.org/10.1016/j.jenvman.2016.08.036>

Pullen, S., & Perkins, A. (1995). *Energy use in the urban environment and its greenhouse gas implications*. <https://www.osti.gov/etdeweb/biblio/394403>

Qualitätsverband Kunststofferzeugnisse e.V., Qualitätsverband Kunststofferzeugniss e.V. (QKE) & European PVC Window Profiles and Related. (2016). *Environmental Product Declaration of PVC-U plastic windows with the dimensions 1.23 x 1.48 m and insolated double-glazing* (Environmental Product Declaration EPD-QKE-20150313-IBG1-EN). Institut Bauen und Umwelt e.V. (IBU).

Rackham, J. W., Couchman, G. H., & Hicks, S. J. (2009). *Composite slabs and beams using steel decking: Best practice for design and construction*.

Ramesh, T., Prakash, R., & Shukla, K. K. (2010). Life cycle energy analysis of buildings: An overview. *Energy and Buildings*, 42(10), 1592–1600. <https://doi.org/10.1016/j.enbuild.2010.05.007>

Rodriguez, B. X., Huang, M., Lee, H. W., Simonen, K., & Ditto, J. (2020). Mechanical, electrical, plumbing and tenant improvements over the building lifetime: Estimating material quantities and embodied carbon for climate change mitigation. *Energy and Buildings*, 226, 110324. <https://doi.org/10.1016/j.enbuild.2020.110324>

RSMeans. (n.d.). *Square Foot Estimate*. Retrieved May 2, 2022, from <https://www.rsmeans.com/>

Scheuer, C., Keoleian, G. A., & Reppe, P. (2003). Life cycle energy and environmental performance of a new university building: Modeling challenges and design implications. *Energy and Buildings*, 35(10), 1049–1064. [https://doi.org/10.1016/S0378-7788\(03\)00066-5](https://doi.org/10.1016/S0378-7788(03)00066-5)

Sika AG. (n.d.). *Gravel Ballasted Roofs*. Retrieved March 17, 2022, from <https://gcc.sika.com/en/construction/roofing/gravel-ballasted-roofs.html>

SimaPro (9.2.0.2). (n.d.). [Computer software]. PRe sustainability.

Simonen, K., Drogue, B. R., Strain, L., & McDade, E. (2017). *Embodied Carbon Benchmark Study: LCA for Low Carbon Construction* [Technical Report]. University of Washington. <https://digital.lib.washington.edu:443/researchworks/handle/1773/38017>

SketchUp Pro 2021 (21.1.332 64-bit). (2021). [Computer software]. Trimble Inc.

Stephan, A., Crawford, R. H., & de Myttenaere, K. (2013). A comprehensive assessment of the life cycle energy demand of passive houses. *Applied Energy*, 112, 23–34. <https://doi.org/10.1016/j.apenergy.2013.05.076>

- Thormark, C. (2006). The effect of material choice on the total energy need and recycling potential of a building. *Building and Environment*, 41(8), 1019–1026.
<https://doi.org/10.1016/j.buildenv.2005.04.026>
- United States Environmental Protection Agency (EPA). (2022). *Emissions & Generation Resource Integrated Database (eGRID)*, 2020. Office of Atmospheric Programs, Clean Air Markets Division. <https://www.epa.gov/egrid>
- U.S. Department of Energy, Building Technologies Office. (2022, March 31). *Status of State Energy Code Adoption—Commercial | Building Energy Codes Program*.
<https://www.energycodes.gov/status/commercial>
- U.S. Energy Information Administration (EIA). (2022). *U.S. energy consumption by source and sector, 2021*.
- U.S. Green Building Council. (2013). *LEED v4: Reference Guide for Building Design and Construction*. U.S. Green Building Council.
- Vahidi, E., Kirchain, R., Burek, J., & Gregory, J. (2021). Regional variation of greenhouse gas mitigation strategies for the United States building sector. *Applied Energy*, 302, 117527.
<https://doi.org/10.1016/j.apenergy.2021.117527>
- Venkatraj, V., Dixit, M. K., Yan, W., & Lavy, S. (2020). Evaluating the impact of operating energy reduction measures on embodied energy. *Energy and Buildings*, 226, 110340.
<https://doi.org/10.1016/j.enbuild.2020.110340>
- Venta, G. J., & Eng, P. (2001). Cradle to gate life cycle inventory for exterior stucco finishes. *Athena Sustainable Institute, Ottawa*.
- Waldman, B., Huang, M., & Simonen, K. (2020). Embodied carbon in construction materials: A framework for quantifying data quality in EPDs. *Buildings and Cities*, 1(1), 625–636.
<https://doi.org/10.5334/bc.31>
- Wan, H., Cao, T., Hwang, Y., Radermacher, R., Andersen, S. O., & Chin, S. (2021). A comprehensive review of life cycle climate performance (LCCP) for air conditioning systems. *International Journal of Refrigeration*, 130, 187–198.
<https://doi.org/10.1016/j.ijrefrig.2021.06.026>
- Wernet, G., Bauer, C., Steubing, B., Reinhard, J., Moreno-Ruiz, E., & Weidema, B. (2016). The ecoinvent database version 3 (part I): Overview and methodology. *The International Journal of Life Cycle Assessment*, 21(9), 1218–1230. <https://doi.org/10.1007/s11367-016-1087-8>
- WUFI Plus* (3.2.0.1). (n.d.). [Computer software]. Fraunhofer IBP.
- YKK AP America. (2015). *Environmental Product Declaration of Aluminum Window Systems* (4786832322.107.1). UL Environment.
- Zhang, J., Rosenberg, M. I., Lerond, J., Xie, Y., Nambia, C., Chen, Y., Hart, R., Halverson, M. A., Maddox, D., & Goel, S. (2021). *Preliminary Energy Savings Analysis: ANSI/ASHRAE/IES*

Standard 90.1-2019 (DOE/EE-2345). U.S. Department of Energy, Office of Energy Efficiency & Renewable Energy. <https://doi.org/10.2172/1131375>

Figure 1: Adapted images from (Banham, 1984) showing two different historical approaches to shelter.	2
In a) the traditional case, the carbon needed to sustain the fire is much greater than that needed to build the tent.	
In b) the high-efficiency case, the smaller and cleaner-burning fire actually emits less carbon over its lifetime than the embodied carbon in the tentpoles and canvas.	
Figure 2: 3D model of case study building, courtesy of Gowri et al. (2007)	3
Figure 3: Map of reference cities with climatic summaries	4
Figure 4: Diagrams of four principal energy simulation cases: a) Base case – ASHRAE 90.1-2004 b) Regenerative Mode – Code envelope with PHIUS equipment c) Conservative Mode – PHIUS envelope with code equipment d) Combined – PHIUS envelope and equipment. All diagrams were laid out by Adam Yarnell and executed by Bianca Seong	8
Figure 5: Cumulative emissions six decarbonization scenarios applied to the eGRID US-Average	9
Figure 6: LCA data quality. Percentages are based on the number of components with individual data sources across all eight cases	9
Figure 7: Key inherited changes in constructing code cases (above) and Passive House cases (below)	9
Figure 8: Box and whiskers plot of the reference scenario. The table on the left lists the selected data filters, and the legend above shows the most important attributes of each case	9
Figure 9: Average life-cycle emissions for the eight case (four code, four Passive House) using the reference scenario data filters	9
Figure 10: Reference scenario comparison of the lowest-emitting code case and highest-emitting Passive House case using initial grid intensities set to a) the U.S. average and b) specific regional grids	9
Figure 11: Comparison of gas and electric cases with a) a high-carbon electric grid and b) a rapidly decarbonized grid	9
Figure 12: Comparison of a low-embodied-carbon code case with Passive House cases in a) moderate and b) idealized scenarios	9
Figure 13: Relative contribution of MEP equipment (embodied carbon and refrigerants) to life-cycle emissions in a rapidly-decarbonized scenario	9
Figure 14: Relative contribution of refrigerants to life-cycle emissions in a high impact scenario	9
Figure 15: Annual grid emissions (kgCO ₂ e/kWh consumed) for an eGRID average grid (US-Average) and four subregions for six decarbonization scenarios: a) business-as-usual b) 50% by 2050 c) 80% by 2050 d) 100% by 2050 e) 80% by 2035, 100% by 2050 f) 100% by 2035	Appx. B
Figure 16: Figure 16: Decision map for the eight life-cycle emissions cases in the study	Appx. C

Table 7: Properties of analyzed systems for refrigerant impact study

System	ASHP	HPWH	Split AC
Reference Product	Mitsubishi M-Series MSZ-FH06NA & MUZ-FH06NA	Aquanext Plus 200	Mitsubishi MSY-GL09NA & MUY-GL09NA
Baseline	R410A	R134a	R410a
High GWP	R404a	R410A	R404a
Lower GWP	R32	R513A	R32
Lowest GWP	R1234ze	CO2	R1234ze
Refrigerant Charge per Unit (kg)		1.162330448	1.344
Capacity	2.55 kW	N/A	2.64 kW
Service Life		25	25
Sources	Mitsubishi Electric Trane HVAC US LLC, 2020; Jin et al., 2016; Systemair srl, n.d.; Sekban, 2018; One Click LCA, n.d.	Ariston Thermo Group & Chaffoteaux, 2016; Hudon et al., 2012; Nyle Systems, LCC, 2021; Eco2 Systems LLC, 2021; One Click LCA, n.d.	Mitsubishi Electric Trane HVAC US LLC, 2019; Jin et al., 2016; Pham & Rajendran, 2012; Sekban, 2018; One Click LCA, n.d.

Table 8: Leakage and EOL loss assumptions for a) air-source heat pump and heat pump water heater and b) split air conditioning system

a)	Scenario	Annual Leakage	EOL Losses	Service Life	B1 Impacts	Sources
	Low	1.00%	1.00%	25	26.00%	George, 2019; One Click LCA, n.d.
	Baseline	3.80%	2.00%	25	97.00%	George, 2019; One Click LCA, n.d.
	High	6.00%	10.00%	25	160.00%	George, 2019; One Click LCA, n.d.

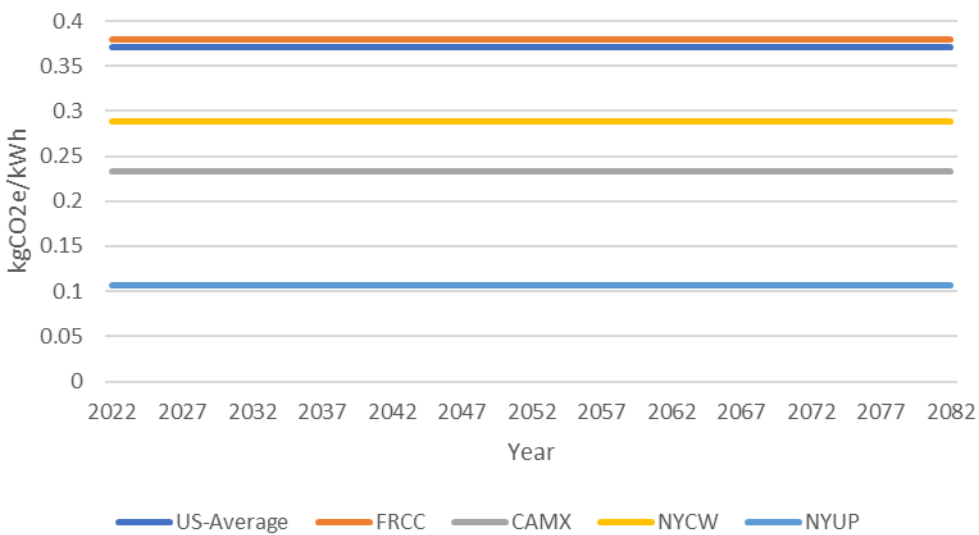
b)	Scenario	Annual Leakage	EOL Losses	Service Life	B1 Impacts	Sources
	Low	2.00%	1.39%	25	51.39%	George, 2019; One Click LCA, n.d.
	Baseline	7.60%	2.78%	25	192.78%	George, 2019; One Click LCA, n.d.
	High	12.00%	13.92%	25	313.92%	George, 2019; One Click LCA, n.d.

Table 9: Life-cycle impacts per specified refrigerant

Refrigerant	Devices	100-year GWP	A1-A3 (kgCO2e)	Sources
R410A	ASHP, AC	2087.5	8.063	California Air Resources Board (CARB), 2022; Bundesministerium für Wohnen, Stadtentwicklung und Bauwesen, 2021
R404a	ASHP	3921.6	8.381	California Air Resources Board (CARB), 2022; Bundesministerium für Wohnen, Stadtentwicklung und Bauwesen, 2021
R134a	HPWH, AC	1430	8.793333333	California Air Resources Board (CARB), 2022; Bundesministerium für Wohnen, Stadtentwicklung und Bauwesen, 2021
CO2	HPWH	1	8.793333333	California Air Resources Board (CARB), 2022; Bundesministerium für Wohnen, Stadtentwicklung und Bauwesen, 2021
R1234ze	ASHP	1	8.793333333	California Air Resources Board (CARB), 2022; Bundesministerium für Wohnen, Stadtentwicklung und Bauwesen, 2021
R32	ASHP, AC	675	8.793333333	California Air Resources Board (CARB), 2022; Bundesministerium für Wohnen, Stadtentwicklung und Bauwesen, 2021
R513A	HPWH	629.76	8.793333333	California Air Resources Board (CARB), 2022; Bundesministerium für Wohnen, Stadtentwicklung und Bauwesen, 2021

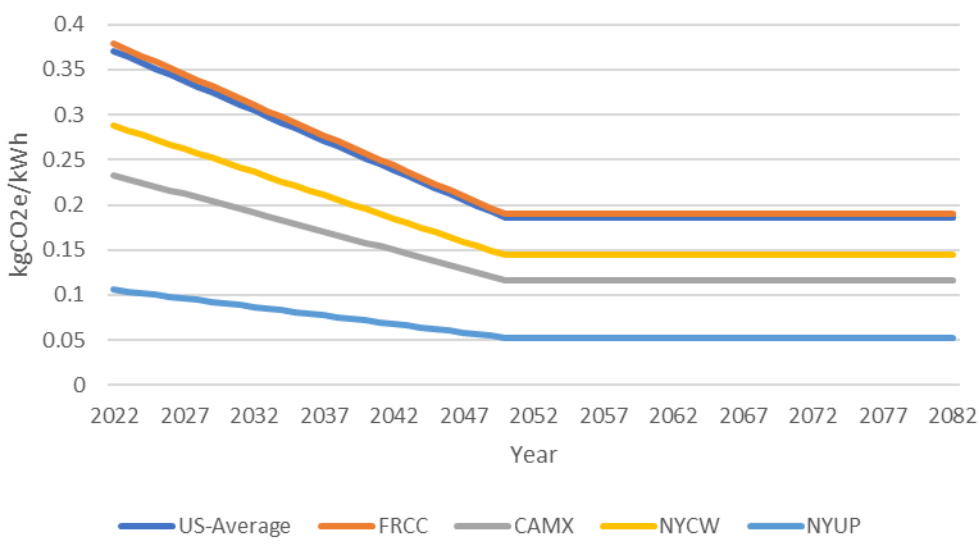
a)

Business as Usual

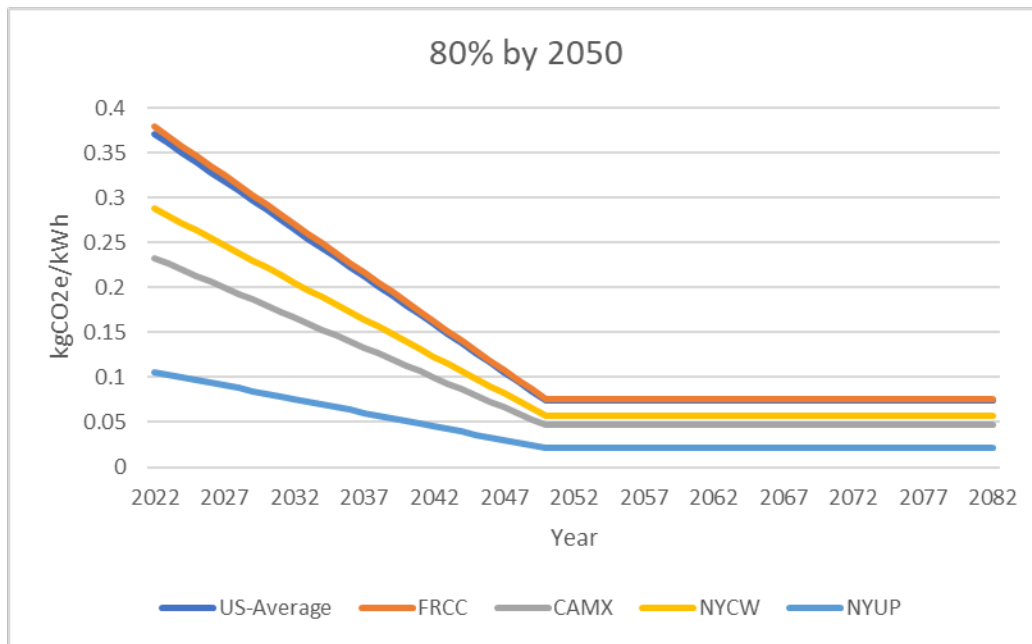


b)

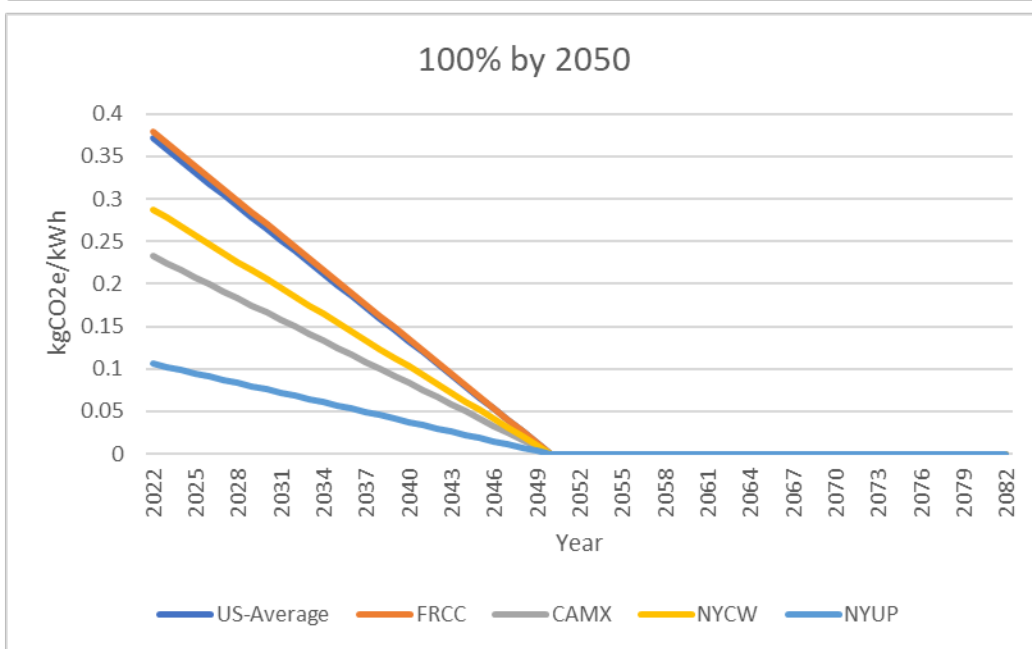
50% by 2050



c)

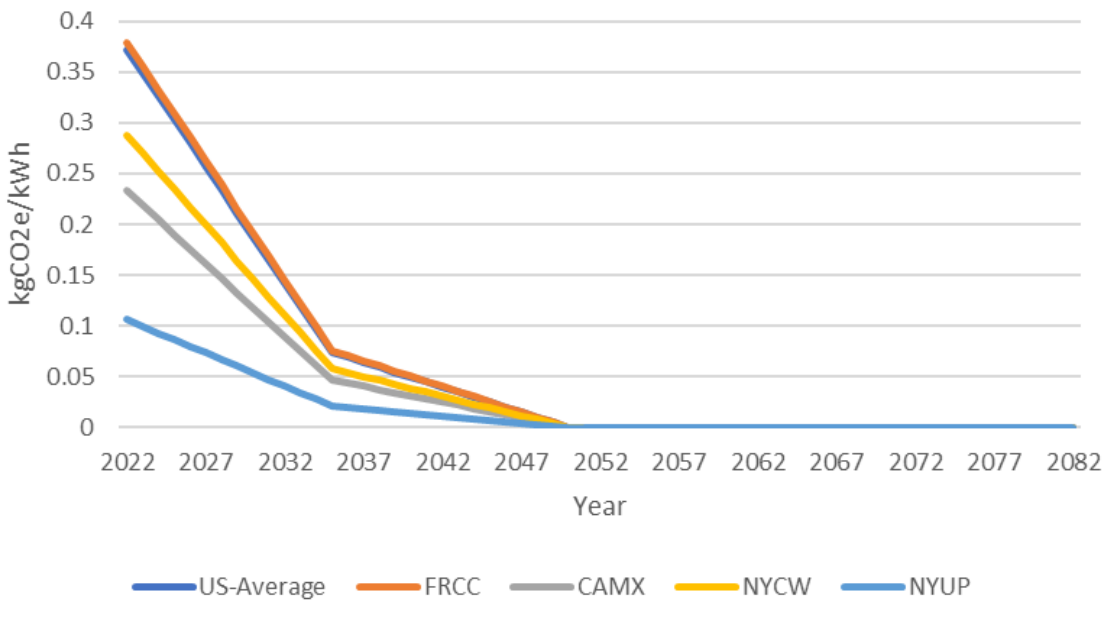


d)



e)

80% by 2035, 100% by 2050



f)

100% by 2035

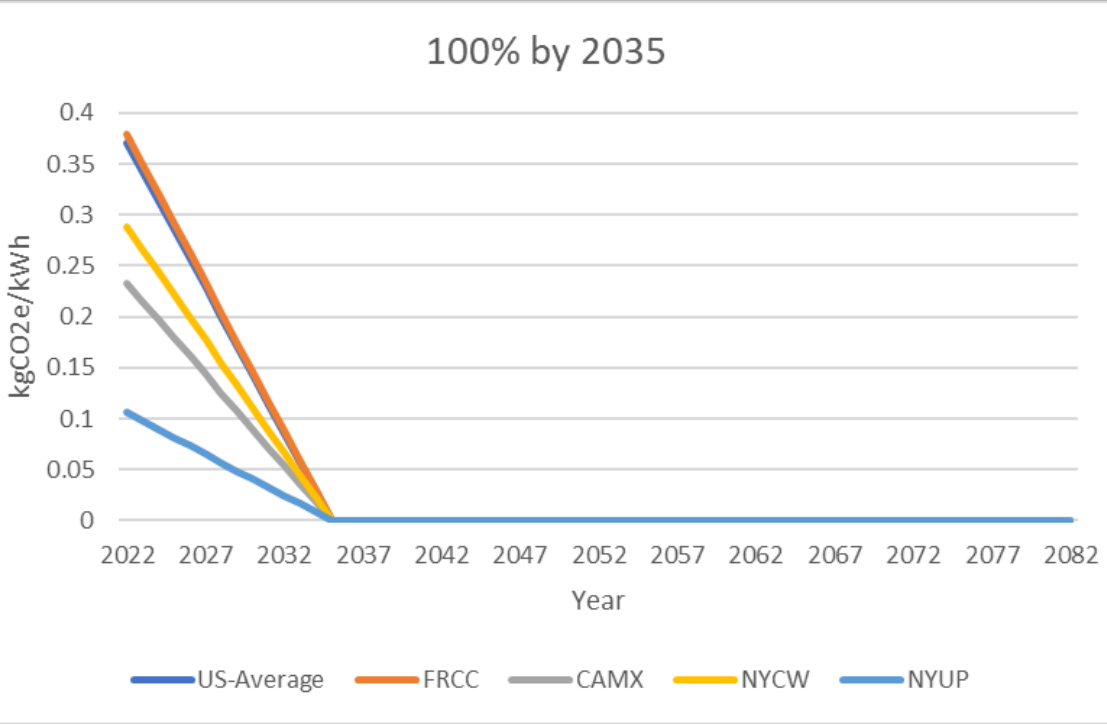


Figure 15: Annual grid emissions (kgCO₂e/kWh consumed) for an eGRID average grid (US-Average) and four subregions for six decarbonization scenarios: a) business-as-usual b) 50% by 2050 c) 80% by 2050 d) 100% by 2050 e) 80% by 2035, 100% by 2050 f) 100% by 2035.

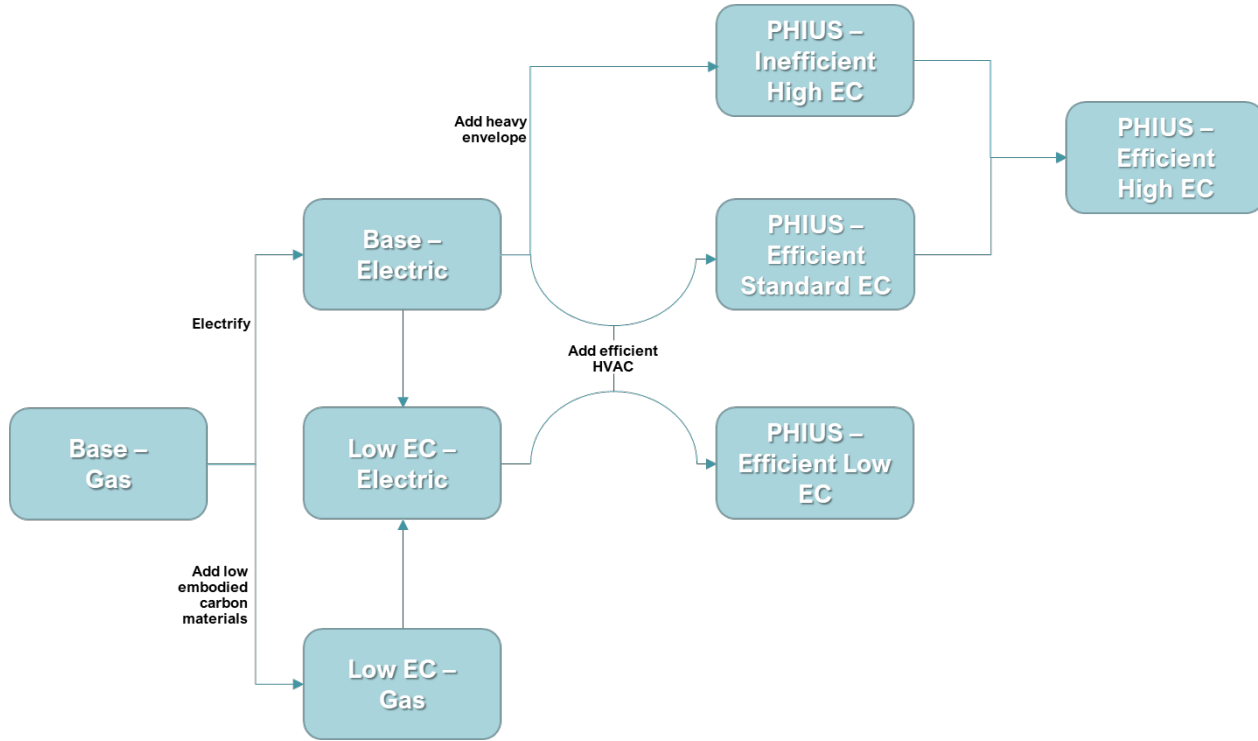


Figure 16: Decision map for the eight life-cycle emissions cases in the study.

Table 10: ENERGY STAR equipment for a) higher-internal-loads cases ("PHIUS – Inefficient High EC") and b) low-internal-loads cases ("PHIUS - Efficient Low EC", "PHIUS - Efficient Standard EC", and "PHIUS - Efficient High EC")

a)	Appliance	Description	Energy Use (kWh/yr)	Energy Use (kWh/d)	Energy Use (kWh/use)	MEF	CEF	Moisture Sensor	Capacity (m3)	Reference Product or Source
Clothes Washer	Top Load	220	0.602739726	N/A	2.06	N/A	N/A	0.127	LG WT7100C*	
Refrigerator	Bottom Freezer, No Ice Maker	400	1.095890411	N/A	N/A	N/A	N/A	0.269	Samsung BRB100033**	
Dryer	Electric Standard Ventless	N/A	N/A	N/A	N/A	3.93	Yes	0.127	Summit LD2444	
Dishwasher	Compact	203	N/A	N/A	N/A	N/A	N/A	N/A	Comfee CDC22P1***	
Kitchen Cooking	Quartz Ceramic Halogen	N/A	N/A	0.22	N/A	N/A	N/A	N/A	WUFI Passive; also see Livchak, et al, 2019	

b)	Appliance	Description	Energy Use (kWh/yr)	Energy Use (kWh/d)	Energy Use (kWh/use)	MEF	CEF	Moisture Sensor	Capacity (m3)	Reference Product or Source
Clothes Washer	Front Load	50	0.136986301	N/A	2.76	N/A	N/A	0.125	Electrolux ELFW7337***	
Refrigerator	Top Freezer, No Ice Maker	283	0.775342466	N/A	N/A	N/A	N/A	0.286	Insignia NS-RTM10BK2	
Dryer	Electric Standard Ventless	236	0.646575342	N/A	N/A	10.4	Yes	4.5	Insignia NS-FDRE44W1	
Dishwasher	Compact	113	N/A	N/A	N/A	N/A	N/A	N/A	Fisher & Paykel DD24STX6I1	
Kitchen Cooking	Induction	N/A	N/A	0.2	N/A	N/A	N/A	N/A	WUFI Passive, n.d.; also see Livchak et al, 2019	